BTO 2017.007 | March 2017

BTO rapport

Subsurface Iron Removal

Field tests at Pumping Station Corle

KWR Watercycle Research Institute

BTO

Subsurface Iron Removal: Field tests at Pumping Station Corle

BTO 2017.007| March 2017

Opdrachtnummer
400378

Projectmanager
dr. Klaasjan Raat

Opdrachtgever
BTO – Speerpuntonderzoek

Kwaliteitsborger(s)
Prof. dr. Pieter J. Stuyfzand

Auteur(s)
Beatriz de la LomaM.Sc., dr. Niels Hartog

Verzonden aan
drs. Martin de Jonge (Vitens)

Jaar van publicatie
2014

Meer informatie
prof.dr. W. van Vierssen
T
E

Keywords
Iron and Manganese removal, modelling

PO Box 1072
3430 BB Nieuwegein
The Netherlands

T +31 (0)30 60 69 511
F +31 (0)30 60 61 165
E info@kwrwater.nl
I www.kwrwater.nl

KWR Watercycle Research Institute

BTO *Managementsamenvatting*

Haalbare efficiëntie van ondergrondse ontijzering is beter in te schatten en te verhogen, wat bijdraagt grotere operationele efficiëntie

Auteur(s) Beatriz de La Loma González, MSc., Dr. Niels Hartog

Veldproeven met twee putten in puttenveld Corle (Vitens) zijn uitgevoerd om de ontijzeringsefficiëntie te vergroten. Bij de goed presterende put PP3 is een twee keer zo groot als normaal volume zuurstofrijk water geïnjecteerd, alvorens weer te onttrekken. Omdat de condities voor ondergronds ontijzeren verbeteren met het aantal opeenvolgende ontrekkingscycli bleek de operationeel haalbare efficiëntie beduidend hoger (1:41) dan de efficiëntie waarop de huidige bedrijfsvoering is gebaseerd (1:23). Bij de slecht presterende PP10 is een verdunde permanganaatoplossing geïnjecteerd, gevolgd door zuurstofrijk water. Oxidatieve voorbehandeling van de bodem verhoogde de efficiëntie in de slecht presterende PP10 van 1:9 naar 1:11, maar de maximaal haalbare efficiëntie werd beperkt door de relatief hoge ijzerconcentraties in het diepe deel van de aquifer. Vitens is op basis van deze inzichten een optimalisatietraject gestart om de (operationele) efficiëntie voor andere putten en winlocaties te verhogen.

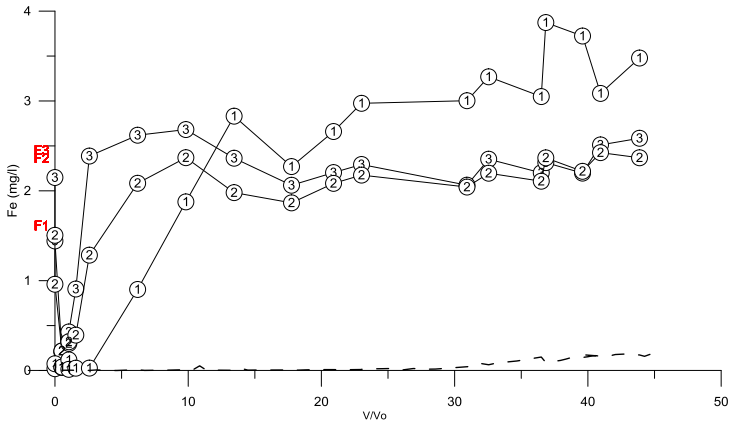

Fig 1. Verandering in de ijzerconcentraties in het opgepompte water en in de aquifer na injectie van 4000 m³ zuurstofrijk water in put PP3. V/Vo is de verhouding tussen het onttrokken en het geïnjecteerde volume. Stippellijn: ijzerconcentratie van het onttrokken (ruw) water. Doorlopende lijn: ijzerconcentraties in waarnemingsfilters (1, 2 en 3) op 5 meter afstand van de put. Concentraties gemeten voor het experiment zijn links van de y-as gemarkeerd. F1 =bovenste filter waarnemingsput, F2 = middelste filter en F3 = diepste filter

Belang: hogere verwijderingsefficiëntie verlaagt operationele kosten

Ondergrondse ontijzering wordt reeds enkele decennia ingezet voor verlaging van de ijzerconcentraties in het opgepompte water uit puttenveld Corle. De efficiëntie van ondergrondse ontijzering, uitgedrukt als de verhouding tussen geïnjecteerd volume zuurstofrijk water en onttrokken volume ijzerarm water, varieert sterk tussen de verschillende winvelden en pompputten. Achterhalen waarom de variatie zo groot is en daardoor inzicht krijgen in de mogelijkheden om de efficiëntie te

Meer informatie
Beatriz de la Loma González
T +31 30 606 9646
E beatriz.dela.lomagonzalez@kwrwater.nl

KWR
PO Box 1072
3430 BB Nieuwegein
The Netherlands

KWR Watercycle Research Institute

vergroten biedt uitzicht op een verlaging van de operationele kosten van (ondergrondse) ontijzering.

Aanpak: veldproeven met en zonder toevoeging van permanganaat

Twee putten in winveld Corle zijn gebruikt voor veldproeven: de goed presterende PP3 en PP10, die een lage ontijzeringsefficiëntie heeft. Bij beide putten zijn eerst op enige afstand waarnemingsputten geplaatst. Van het sediment dat bij de aanleg van deze waarnemingsputten werd opgeboord, is de achtergrondreactiviteit bepaald. Vervolgens zijn twee veldexperimenten uitgevoerd. Bij de goed presterende put is een twee keer zo groot volume zuurstofrijk water (4000 m^3) als normaal geïnjecteerd alvorens met de onttrekking te beginnen. Bij de slecht presterende PP10 is een verdunde natriumpermanganaat ($NaMnO_4$) oplossing toegevoegd aan de eerste 2000 m^3 geïnjecteerd zuurstofrijk water, gevolgd door nog eens 2000m^3 zuurstofrijk water zonder permanganaat, om de hypothese te testen dat deze sterke oxidant de achtergrondreactiviteit van het sediment bij PP10 kan verminderen en zo de efficiëntie kan verhogen. IJzer- en mangaanconcentraties (Figuur 1), overige macrochemie en sporenelementen zijn nauwkeuring gemonitord voor, tijdens en na beide experimenten.

Fig 2. Paars water (met permanganaat) wordt opgepompt uit een waarnemingsput

Resultaten: oxidatieve behandeling kan operationele efficiëntie verhogen, maar veel ijzer verlaagt dit effect

Beide putten konden na de experimenten met hogere ontijzeringsefficiëntie worden bedreven. Ook waren de mangaanconcentraties in het opgepompte water aanvankelijk lager door adsorptie aan tijdens de injectie gevormde mangaanoxides. De mangaan-concentraties namen echter in beide putten weer toe gedurende verdere onttrekking, waarschijnlijk doordat de gevormde mangaanoxides reduceren door toestromend ijzer(II), wat leidt tot een verder vertraagde ijzerdoorbraak. De operationeel haalbare efficiëntie bleek voor PP3 beduidend hoger (1:41) dan het uitgangspunt voor de huidige bedrijfsvoering (1:23). Dit wordt toegeschreven aan de steeds gunstigere geochemische condities die ontstaan tijdens het (langjarig) verloop van meerdere injectie-ontrekkingscycli.

De injectie van permanganaat in PP10 resulteerde in een toename van de ontijzeringsefficiëntie van 1:9 naar 1:11. De door de voorbehandeling gevormde mangaanoxiden veroorzaakten slechts een beperkte verbetering van de ondergrondse mangaan-verwijdering omdat ijzer (te) sterk concurreert voor de ingebrachte zuurstof. De reductie van de mangaanoxiden door opgelost ijzer in het instromende grondwater leidde tot een tijdelijke verhoging van de mangaanconcentraties. Daarom heeft een andere sterke oxidant (zoals peroxide of persulfaat) de voorkeur als middel om de ondergrondse ontijzering te verbeteren. De operationele efficiëntie die voor PP10 gehaald kan worden, wordt beperkt door de relatief hoge ijzerconcentraties in het diepe deel van de aquifer. Daardoor wordt een groter deel van het hoger ingebrachte zuurstof niet benut voor ijzeroxidatie.

Implementatie: ijzer bepalen per put belangrijk voor optimalisatie ondergrondse ontijzering

Op basis van de ijzerconcentraties in het onttrokken water kan de maximaal haalbare efficiëntie worden bepaald. Het is daarbij belangrijk de ijzerconcentraties in het grondwater *per put* te bepalen en na te gaan of deze over de lengte van het filter varieert. Bepalen van de maximaal haalbare efficiëntie vergt een inschatting van de reactiviteit van het sediment. Oxidatieve behandeling kan bijdragen aan het verbeteren van de efficiëntie, met name voor locaties met relatief lage ijzerconcentraties. De efficiëntie van ondergronds ontijzeren neemt daarbij toe met het aantal injectie-onttrekkingscycli. Vitens heeft op basis van deze inzichten een optimalisatietraject gestart om de (operationele) efficiëntie voor andere putten en winlocaties te verhogen.

Rapport

Dit onderzoek is beschreven in het rapport *Subsurface Iron Removal. Field tests at Pumping Station Corle* (BTO-2017.007).

Meer informatie
Beatriz de la Loma González
T +31 30 606 9646
E beatriz.dela.lomagonzalez@kwrwater.ml

KWR
PO Box 1072
3430 BB Nieuwegein
The Netherlands

Content

1	Introduction	7
1.1	Field pilots subsurface iron removal at Corle pumping station	7
2	Set-up of field pilots	9
2.1	Description of well locations 3 and 10	9
2.2	Sediment sampling and monitoring filter installation	10
2.3	Sediment characterization	13
2.4	Experimental cycles during the field pilots	14
2.5	Online Monitoring	15
2.6	Groundwater sampling and analysis	15
2.7	Permanganate application in well 10	15
3	Results and Discussion	17
3.1	Sediment characterization	17
3.2	Field pilot at well 3	19
3.2.1	Online monitoring	19
3.2.2	Observed iron and manganese concentrations	20
3.3	Field pilot at well 10	24
3.3.1	Online monitoring	25
3.3.2	Observed iron and manganese concentrations	26
3.4	Controls on iron and manganese concentrations	33
3.5	Fate and impact of permanganate application	37
3.5.1	Impact of permanganate application on abstracted groundwater	37
3.5.2	Impact of permanganate application on aquifer sediment	39
3.6	Removal Efficiencies during Subsurface Iron Removal	39
3.6.1	Observed removal efficiencies during and after field pilots	39
3.6.2	Implications for optimization of SIR efficiencies	41
4	Conclusions	44
5	Literature	46

1 Introduction

The '*speerpuntonderzoek* ' project named 'Removal of iron and manganese in the drinking water chain: from estimation to control (*'Ontijzering en ontmanganing in de drinkwaterketen: van schatten naar sturen'*) aims for a better understanding and prediction, as well as a more efficient operation, of the aboveground and underground removal of iron and manganese. Within this project the efficiency and operational controls of Subsurface Iron Removal (SIR) were investigated for drinking water company Vitens using both modeling and field tests. This research was conducted at pumping station Corle and is described in this report.

The efficiency of SIR systems strongly depends on the location characteristics. Iron concentrations in groundwater and oxygen concentrations in the infiltrating water are known to determine the maximal (theoretical) efficiency. With SIR, oxygen is introduced to oxidize ferrous iron. However, as part of the injected oxygen is lost in reactions with the sediment, this decreases the SIR efficiency. Reactive transport modelling of historical pilots including sediment reactivity has already been performed within this "speerpuntonderzoek" by (de la Loma and Hartog, 2016). These modelling experiences revealed that sediment reactivity was location-specific and a main factor in the efficiency evolution. Differences in sediment reactivity can also explain why there are significant differences between the recovery efficiencies of locations with similar water compositions (iron concentrations and pH of native groundwater). In addition, these modelling results indicated that evolution of efficiency strongly depends on how the sediment reactivity decreases over time and on the initial composition of iron hydroxides. These results suggest that it is possible to optimize the operational efficiency per location based on these factors. This potential for optimization was tested for wells at pumping station Corle.

1.1 Field pilots subsurface iron removal at Corle pumping station

The location selected for the field-tests is Corle. On this location, SIR has been taking place for decades and currently pure oxygen is being used to increase the oxygen concentration (up to 20 mg/l) in the injected water to raise the SIR efficiency. Two wells in the SIR pilot (coded 3-20 and 10-25) were selected for testing. For these two wells the options for location-specific optimization are studied through the following experiments:

Experiment 1. Injection of a double volume (4000 m^3) of oxygen-rich water in a well with good recovery efficiency (well 3-20). The objective was to obtain information, through the recovered water, on the reactivity of the sediment surrounding the standard volume of injection (2000 m3), that is, the sediment not influenced yet by the SIR system. The SIR efficiency was therefore expected to decrease.

Experiment 2. Injection of a standard volume in well 10-25, a well with low SIR efficiency, but water dosed with $NaMnO_4$ aqueous solution. This reagent is meant to decrease the reactivity of the sediment. The field experiment had the objective to test experimentally how the efficiency can be improved by oxidative treatment of the well proximal zone.

2 Set-up of field pilots

2.1 Description of well locations 3 and 10

There are 12 active SIR wells in well field Corle, the average removal efficiency in the well field is 16.92 (RE = abstracted volume of water with admissible iron concentrations / infiltrated volume of water). However, the efficiency varies strongly per well; the two selected wells for the experiments were the most and the least efficient wells respectively: well 3 with RE =23 and well 10 with RE= 9 (in Figure 2-1: COR-P03-20, COR-P10-25, respectively).

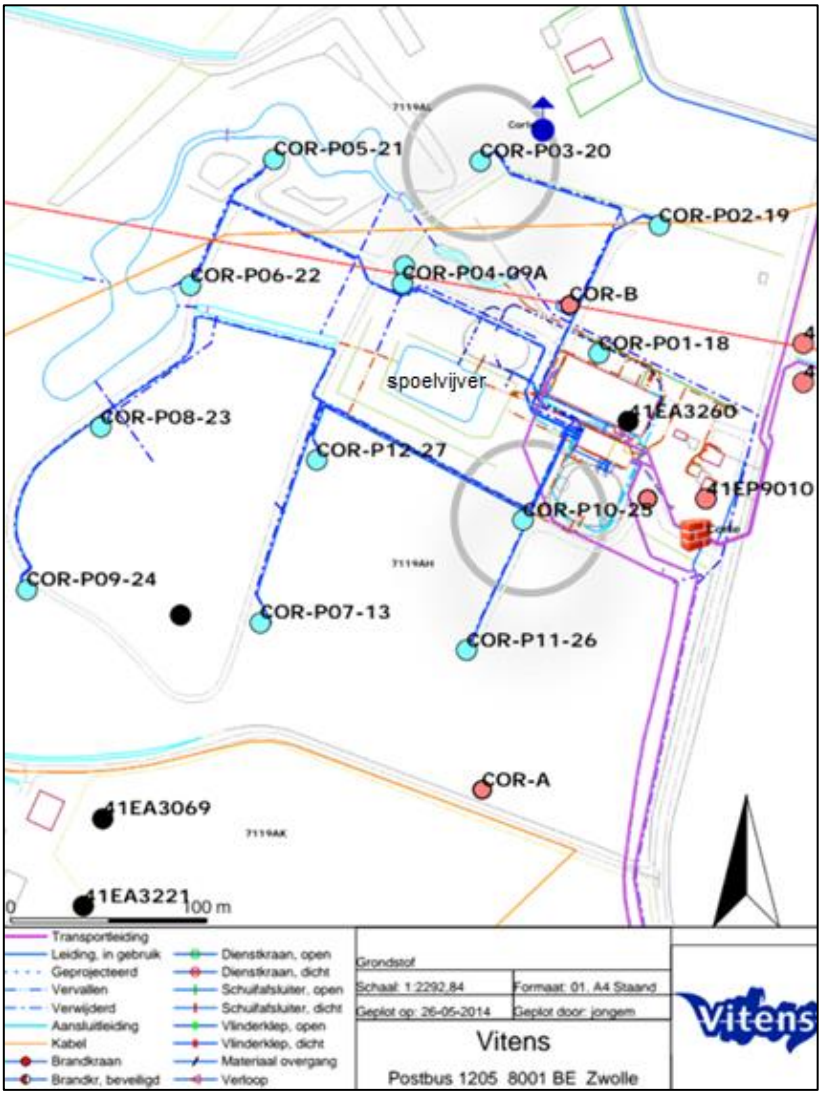

Figure 2-1Technical overview of the well field at location Corle. The grey circles mark the selected wells for the SIR pilot: well 3 (COR-03-20) and well 10 (COR-P10-25). The flushing pond (spoelvijver) is centrally located in the well field.

The pumping wells in well field Corle are screened in the Drente formation with screendepth between 0 and 30m – NAP (*Figure 2-2*). The aquifer mainly consists of coarse sand and is confined by the underlying Breda formation and the overlying Eemklei.

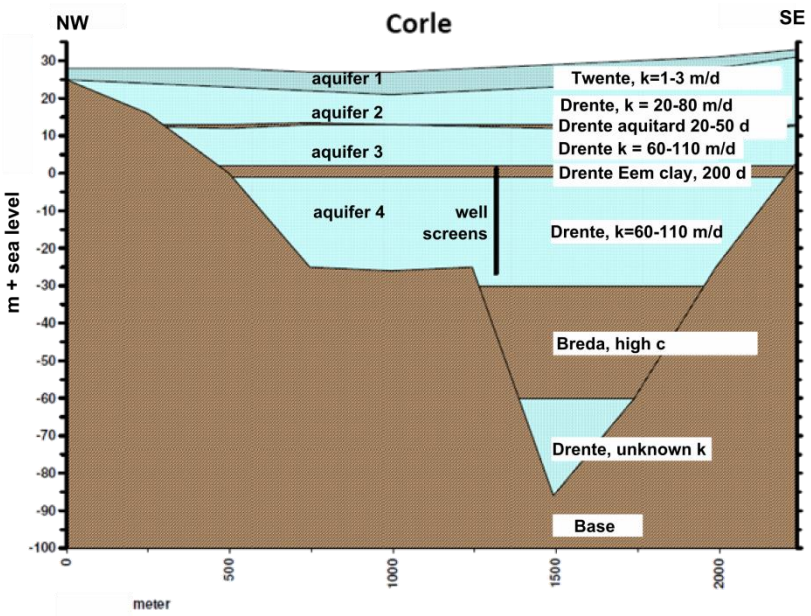

Figure 2-2: Geohydrological cross-section of well field Corle.

The two selected wells have sceen depths averaging at 35 m below surface level, that is around 5 m below NAP (Table 2-1) in a formation mainly composed of sand except for one to two meters of gravel (32 to 33 and 32 to 34m below surface in wells 3 and 10 respectively). These wells were drilled in 1998 and have been functioning since 1999,

Table 2-1 Filter depths of the selected wells for the pilot tests

Well	upper part filter (m-surface)	lower part filter (m-surface)
10	27	39.65
3	31	40.12

2.2 Sediment sampling and monitoring filter installation

As part of the field experiments, one monitoring well was installed at 5 m distance from each of the SIR wells selected. The monitoring wells were positioned approximately at the calculated distance for half an injected pore volume (1000 m3) from the pumping well. This ensured that the infiltrated water would reach the monitoring wells. Each monitoring well was equiped with three 1 m long monitoring screens that were installed at the top, middle and bottom of the pumping well screen (Table 2-2).

Table 2-2: Installed monitoring filters in well 3 and 10

Well number	Bore	Filter	Screen depth (m-surface)	Location (x, y)
3	B41EM001	PB01	31,00–32,00	241.769, 442.040
3	B41EM001	PB02	35,00–36,00	
3	B41EM001	PB03	39,00–40,00	
10	B41EM002	PB01	26,50–27,50	241.791,441.842
10	B41EM002	PB02	33,00–34,00	
10	B41EM002	PB03	39,00–40,00	

To investigate in detail the sediment composition and initial reactivity around the SIR wells, during the drilling 0.3m long sediment cores were taken, with a total of 9 and 13 undisturbed sediment samples distributed over the depth range of the monitoring well screens at wells 3 and 10, respectively. Figure 2–3 and Figure 2–4 show the location of the monitoring screens, the sediment samples and the sediment description over depth. The sediment within the depth range of the SIR well screen consists mainly of sands with a higher gravel contribution around 32–34m deep, coinciding with screen 1 of well P03, and screen 2 of well P10.

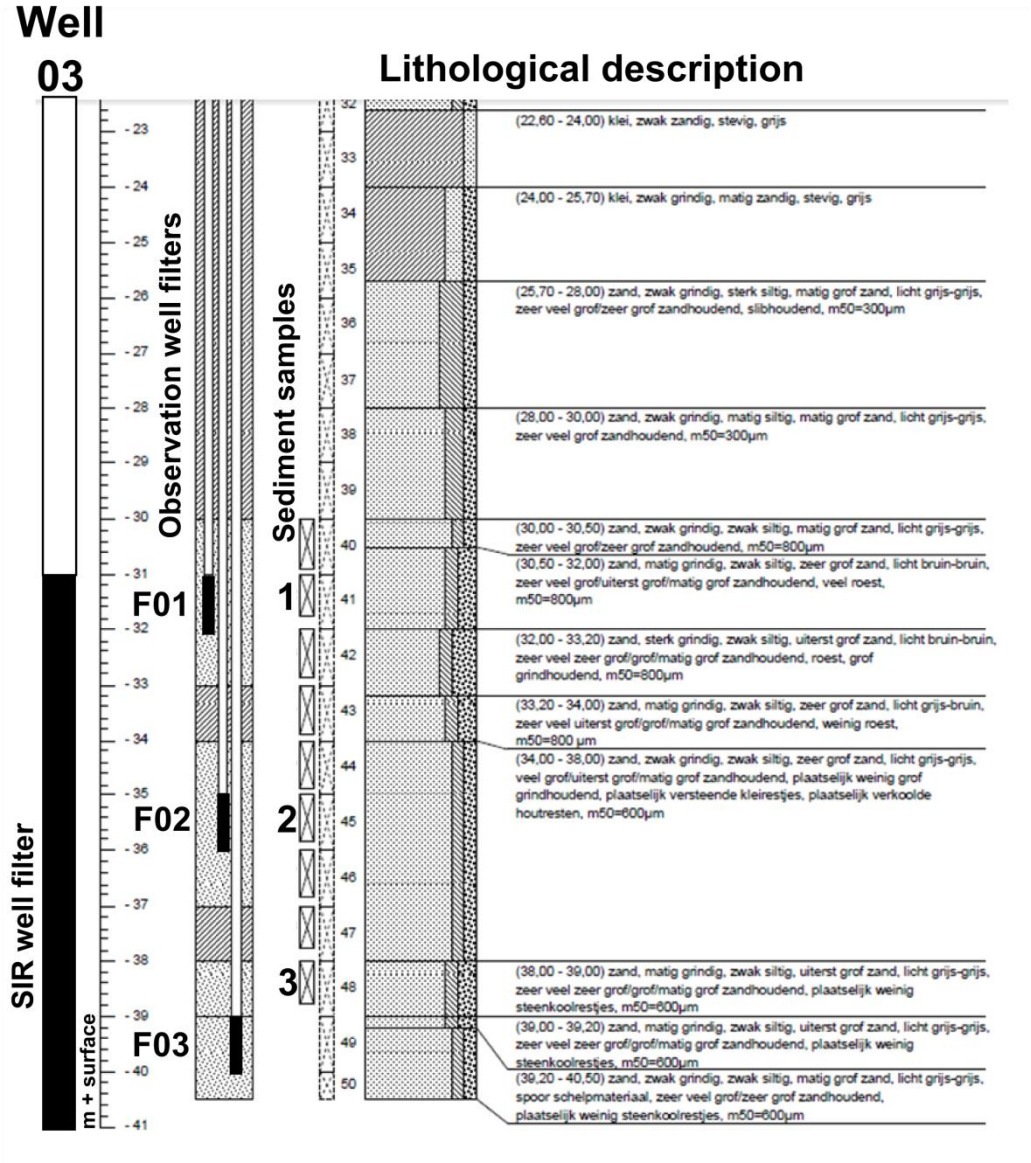

Figure 2-3 Lithology of the aquifer at the monitoring well next to well 03, with the depth of the installed monitoring screens (F01,F02, F03) and the sediment cores chosen for analysis (1-3). At the left of the figure, the depth range of the screen of well 3 is also indicated.

During the drilling the following sediment characteristics were observed: the gravelly sand surrounding the first screen in well 03 showed a significant amount of rust (indicating the presence of iron-hydroxides), meanwhile the second monitoring screen was surrounded by sand containing clay and carbonized wood residues (extra background reactivity). The sand surrounding the third screen contained traces of shell material (calcite) .

The first screen in well 10 was surrounded by silty sand, between the first and the second screen in well 10 there was a layer of gravelly sand with rust and clay residues. The second screen of this well was surrounded by gravelly sand that contained traces of shell material under which there was a coarse sand layer with a significant amounts of rust. The third screen was surrounded by medium-coarse sand with less rust.

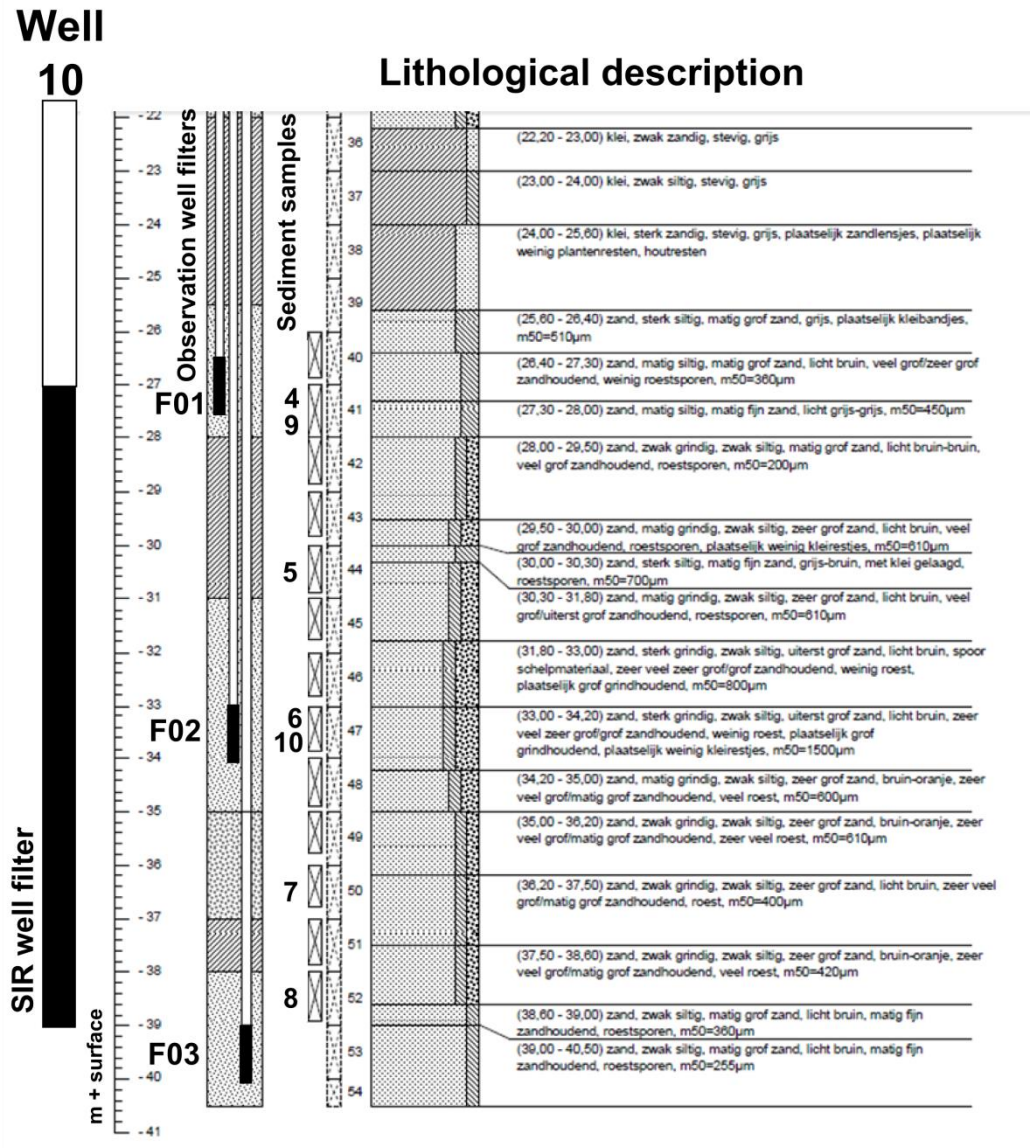

Figure 2-4 Lithology of the aquifer at the monitoring screen beside well 10 with the depth of the installed monitoring screens (F01,F02, F03) and the sediment samples chosen for analysis (4-10). The depth range of the screen of SIR well 10 is also indicated at the left of the figure.

2.3 Sediment characterization

From the 24 undisturbed sediment samples taken (Figure 2-5), 10 representative samples (Table 2-3) were sent to the laboratory for the following sediment analysis: element determination after nitric acid digestion, thermogravimetric analysis (LAM- 066), x-ray fluorescence, CNS analysis and permanganate natural oxidant demand of sediment. Two samples at 27 and 33 m deep of well 10 were treated with 30g/l of permanganate in batch experiments and analyzed after 48h to study the consumption of permanganate and the effect of permanganate treatment on the sediment composition. This was done according to the Standard Test Method for Estimating the Permanganate Natural Oxidant Demand of Soil Aquifer Solids (ASSTM D7262 – 10).

Table 2-3 Selected sediment samples for sediment analysis

Sample nr	Depth	Well	Screen	observations
1	31 - 32 m	P03	PB01	
2	35 - 36 m	P03	PB02	
3	38 - 39 m	P03		
4	27 - 28 m	P10	PB01	
5	30 - 31 m	P10		
6	33 - 34 m	P10	PB02	
7	36 - 37 m	P10		
8	38 - 39 m	P10		
9	27 - 28 m	P10	PB01	Nr 4 after 30 g/ l KMn04
10	33 - 34 m	P10	PB02	Nr 6 after 30 g/ l KMn04

Figure 2-5 Sediment samples wells 3 and 10

2.4 Experimental cycles during the field pilots

The field experiments began in Corle in March 2015 and for each well several infiltration/abstraction cycles were performed.

After infiltrating 4,000 m^3 (80m^3/h) of oxygenated water via well 03, 45 volumes could be recovered (V_{out}/V_{in} = 45) during almost four months until reaching iron concentrations of 0.2mg/l.

In well 10 (original average V_{out}/V_{in} = 9), three main cycles took place; firstly a standard infiltration (80m^3/h) and recovery of 2,000 m^3 (V_{out}/V_{in} = 8.68), and secondlyan infiltration of 1,950m^3 dosed with a sodium permanganate solution (4m^3 Carusol C 40% concentration for potable drinking water applications) followed by an infiltration of 2,000 m^3 of oxygenated

water, with a recovery of 15 volumes (V_{out}/V_{in}) and an iron concentration of 0.01mg Fe/l. In the third cycle, 2,000m^3 of oxygenated water was infiltrated after which 39 times this volume was recovered up to 0.92mg Fe/l. This extensive abstraction took place to allow the abstracted manganese concentrations to decrease.

Table 2-1: Overview experimental cycles

Well	Cycles	Treatment	Infiltrated Volume (m^3)	Elapsed time *(days)	volumes abstracted (m^3)
3	1.Injection	Oxygenated (with O2)	4000	1	
3	1.Abstraction			119	180000
10	1.Injection	Oxygenated (with O2)	2000	1	
10	1.Abstraction			8	17600
10	2.Injection	Permanganate (with O2)	3950	2	
10	2.Abstraction			57	62600
10	3.Injection	Oxygenated (with O2)	2000	1	
10	3.Abstraction			101	78518

** Elapsed time = time (days) abstracting or infiltrating.*

2.5 Online Monitoring

At the start of the recovery online monitoring was performed to track the fast changes in dissolved oxygen, pH, redox potential and electrical conductivity of the abstracted water.

2.6 Groundwater sampling and analysis

The monitoring screens were developed and pumped clean prior to the start of the field pilots. Samples for cation and traceelement analysis (ICP-MS) were acidified in the field for preservation until analysis. Water samples were taken of the injected and abstracted water and of the groundwater from the monitoring screens. The frequency varied from several times per day right after the beginning of the injection or abstraction up to 1 time per week after several weeks of abstraction.

.

2.7 Permanganate application in well 10

A NaMnO4 solution was used to reduce the background reactivity of the aquifer. This permanganage solution is certified for use in potable water production because of its high purity and negligible trace element content (KIWA- certification no. K83927). Four thousand litres (4 IBC's – intermediate bulk containers– of 1 m^3, Figure 2-7) of sodium permanganate solution (40%, 400g/L) were dosed to the 2000m^3 of injected water during the second injection cycle in well 10 (Table 2-1). This resulted in an average injected sodium and permanganate concentration during this cycle of 129 mg/L and 669 mg/L, respectively. However, as the 4000L of permanganate solution could not be dosed continuously during the infiltration, the maximum infiltrated concentrations are expected to be slightly higher. Since the presence of permanganate turns the infiltrated water purple, its infiltration and transport into the aquifer were easily tracked in the monitoring wells (Figure 2-7).

Figure 2-6 Four IBC's of sodium permanganate, dosed to the injected 2000m³ during the second experimental cycle of well 10.

Figure 2-7 Purple water (due to the presence of MnO4) pumped from the 3 screens of the monitoring well 5 m away from well 10.

3 Results and Discussion

This chapter compiles the findings of the field experiments at pumping wells 3 and 10 at Corle. Firstly, the outcomes regarding sediment composition and background reactivity in the surrounding of the wells are described. Secondly, the subsurface iron and manganese removal processes observed in wells 3 and 10 along the different infiltration/abstraction cycles are described. Thirdly, the impact of the permanganate application is discussed and lastly the effects of the experimental cycles on the recovery efficiencies are described together with their implications for SIR optimization.

3.1 Sediment characterization

As described by the modelling performed previously in this project (de la Loma and Hartog, 2016), the removal efficiency of SIR systems will depend greatly not only on the composition of the infiltrated water and groundwater but also on the background reactivity of the aquifer. The natural oxidant demand of the sediment for permanganate is indicative of the aquifer's background reactivity (Table 3-1). The sediment surrounding Well 10 seems to have a higher background reactivity (higher permanganate consumption) than the sediment around well 3 in the second half of the screen length. The sediment at the top first meters around well 3 however, seem to have a higher background reactivity than the top first meters around well 10.

Table 3-1 Permanganate oxidant demand of the undisturbed sediment samples taken from well 3 and 10 in grams of permanganate consumed by kg of sediment per day.

			Permanganate consumption		
			10 g / 1 g KMnO4/kg d	20 g / l g KMnO4/kg d	30 g / 1 g KMnO4/kg d
P03	1	31 – 32 m	2.2	2.6	2.2
P03	2	35 – 36 m	2	3.2	3.2
P03	3	38 – 39 m	4.7	5.5	9.2
P10	4	27 – 28 m	1.5	1.5	2
P10	5	30 – 31 m	0.64	1	1.3
P10	6	33 – 34 m	2	2.1	3.5
P10	7	36 – 37 m	3.4	4.1	4.7
P10	8	38 – 39 m	6	6.6	7

Organic matter and pyrite can play an important role by competing for the oxygen with iron and manganese. These parameters can be calculated based on the determined CNS content, the values of which are within the expected range for sandy aquifer sediments (Table 3-2).

In contrast with the determined natural oxidant demand as measured with permanganate consumption, the percentages of organic matter (based on the content of C) and pyrite in well 3 are higher in the last meters than in well 10. The total pyrite content, however, is not directly related to the its reactivity, since not all might be available for reaction, especially if it is carbonate buffered as the system seems to indicate (described in the results section 3.4).

Also, the reactivity of organic matter depends highly on its composition (Hartog et al., 2005; Hartog et al., 2004), and can vary even within the same formation that these wells are in.

The TGA analysis indicates also that the calcite content varies with depth, with well 10 showing a higher average calcite content than well 3 (Table 3-3). This matches the lithological description observed during the drilling of the monitoring well (Figure 2-4). The calcite content calculated via Ca is in general higher than the calcite content calculated via TGA. This indicates that part of the Ca is not calcite-bound but bound to both silicate minerals and the cation exchanger. Even the TGA derived calcite levels are probably a bit too high, because the weight loss between 550 and 1000oC is partly derived from losses of structurally bound water.

Table 3-2 C and S content of the undisturbed sediment samples, and Al, Mn, Ca and Fe content after nitric acid digestion of the sediment samples. The samples marked with an asterisk ( ) indicate those treated first with $KMnO_4$. The organic matter (BOM), pyrite and calcite content of the sediment is calculated based on these parameters.*

		Depth	Al	Mn	Ca	Fe	C	S	BOM	FeS_2	Calcite
		m	g/kg ds	g/kg ds	g/kg ds	g/kg ds	%	%	%	%	%
P03	1	31 - 32	0.292	0.094	12.5	8.32	0.035	0.042	0.07	0.078	3.125
P03	2	35 - 36	0.234	0.141	36.8	3.72	0.13	1.35	0.26	2.522	9.2
P03	3	38 - 39	0.277	0.211	46.7	4.08	0.41	0.68	0.82	1.2652	11.675
P10	4	27 - 28	0.598	0.213	47	3.33	0.038	0.014	0.076	0.02561	11.75
P10	9*	27 - 28	0.514	0.818	47.3	3.02	0.016	0.017	0.058	0.01639	11.825
P10	5	30 - 31	0.233	0.142	9.83	2.27	0.053	0.037	0.032	0.03154	2.4575
P10	6	33 - 34	0.352	0.401	16.8	4.72	0.061	0.32	0.106	0.06838	4.2
P10	10*	33 - 34	0.505	1.4	12.5	4.42	0.14	0.26	0.054	0.06503	3.125
P10	7	36 - 37	0.5	0.097	25.3	8.88	0.029	0.009	0.122	0.5973	6.325
P10	8	38 - 39	0.445	0.102	34.9	14.4	0.027	0.035	0.28	0.4840	8.725

Table 3-3 Calculated values of calcite content based on the thermogravimetric analysis (TGA) results.

			TGA-Dry residue 105 ° C (%)	TGA - Residue ignition 330 ° C (%)	TGA - Residue ignition 550 ° C (%)	TGA - Residue 1000 ° C (%)	$CaCO_3$ %
P03	1	31 - 32 m	86	85.9	85.6	84.7	2.0468
P03	2	35 - 36 m	85.2	85.1	84.6	82.6	4.5484
P03	3	38 - 39 m	86.2	85.9	85.3	82.1	7.2774
P10	4	27 - 28 m	86.9	86.9	86.5	82.2	9.7791
P10	5	30 - 31 m	88.2	88.2	88	87.4	1.3645
P10	6	33 - 34 m	86.8	86.7	86.4	85.3	2.5016
P10	7	36 - 37 m	82.6	82.4	82.3	75.6	15.2371
P10	8	38 - 39 m	81.5	81.2	80.9	84.4	

3.2 Field pilot at well 3

The initial water quality, measured before the start of the field experiments, at the monitoring screens near well 3 is fresh (EC between 55 and 60) with Ca and HCO_3 as main ions, pH around 7.5 and an iron concentration ranging from 1.6 to 2.45 mg/l (Table 3-4).

Table 3-4 Initial groundwater quality in the monitoring well beside Well 03 and average of the infiltrated water in Well 03 at the 3rd of March of 2015. .

P-03		PB01	PB02	PB03	P03-IN
Sampling date		2-3-2015	2-3-2015	2-3-2015	3-3-2015
Depth (m-surface)		31,00-32,00	35,00-36,00	39,00-40,00	
pH -in situ	pH	7.5	7.6	7.5	7.34
Ca	mg/l	118.3	109.5	112.6	102.98
Cl	mg/l	38.2	42.5	49.5	38.69
DOC	mg/l	1.99	2.28	3.11	
Fe total	mg/l	1.80	2.33	2.41	<0.05
Fe dissolved	mg/l	1.61	2.36	2.45	0.019
EC - 20C	mS/m	60.8	55.6	57.8	56.7
HCO_3	mg/l	171.4	171.5	208.0	234.2
K	mg/l	1.1	1.0	1.7	2.52
Mg	mg/l	6.6	6.2	6.6	7.82
Mn	mg/l	0.30	0.24	0.22	<0.005
Na	mg/l	20.6	14.3	13.2	24.97
NH_4	mg NH4 / l	0.25	0.21	0.15	<0.03
SO_4	mg SO4 / l	164.8	119.8	91.1	90.96
Sr	µg/l	408.5	363.1	593.8	606.7
O_2	mg/l				20

The infiltration of 4000 m^3 oxygen-rich (iron-free) water occurred at a rate of 80m^3/h during approximately two days, after which the water was abstracted again at a rate of around 80 m^3/h during 119 days, abstracting a total of 180000 m^3. The abstracted water in well 3 was continuously monitored and samples were taken of the groundwater in the three monitoring screens as well as of the abstracted water.

3.2.1 Online monitoring

The online monitoring of the abstracted water in well 03 gave insight into the development of oxygen concentrations, pH and EC during the beginning of the recovery.

The oxygen concentrations were high during the first recovery hours and decreased down to 0 mg/l after 22h of abstraction at around half a pore volume (V/V_0= 0.6). The pH in the abstracted water ranged from 6.99 up to 7.47. It decreased during the first abstraction hours after which there was a significant increase and decrease around one abstracted pore volume followed by a steady increase (with several pH peaks -at around 7.4- observed during the whole recovery time that could be related to sampling moments). EC ranged between 63 and 78 ms/m and it fluctuated during the recovery period.

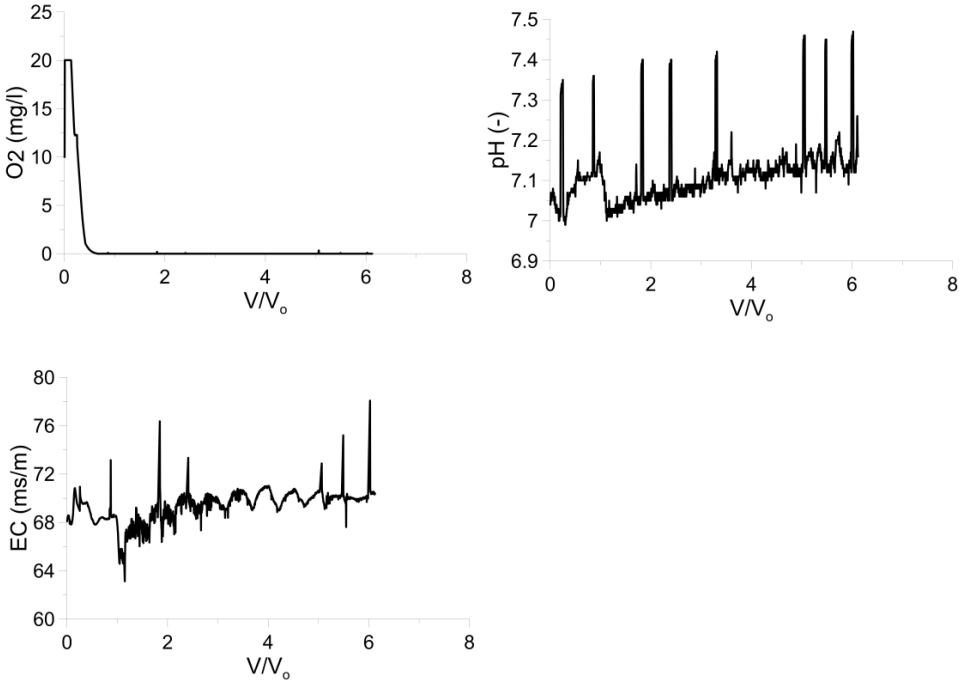

Figure 3-1 Online monitoring performed in well 03

3.2.2 Observed iron and manganese concentrations

Iron

The observed iron concentrations differed between the abstracted water and the groundwater measured in the monitoring well at screens 1,2 and 3 (Figure 3-2). While the iron concentrations at the three monitoring screens relatively rapidly returned to their different background iron concentrations (especially at screens 2 and 3), the abstracted iron concentration remained at much lower levels. This indicates that the iron removal processes were taking place within 5m distance from the abstraction well.

During abstraction, after 6 PV (V/V_0) the iron concentrations in screens 2 and 3 stabilized around the initially measured concentrations (Table 3-4). However, the iron concentration in screen 1 seemed to increase somewhat with time. This however did not affect the iron concentrations in the abstracted water in well 03 as it remained below 0.2 mg/L the whole time. The efficiency achieved was much higher than the normal removal efficiency of the well (45 instead of 23). This contrasts with the reduced efficiency that was expected to result from injecting a larger volume and suggests that the well was operated under a lower efficiency than what was achievable, even when enriching the water with oxygen.

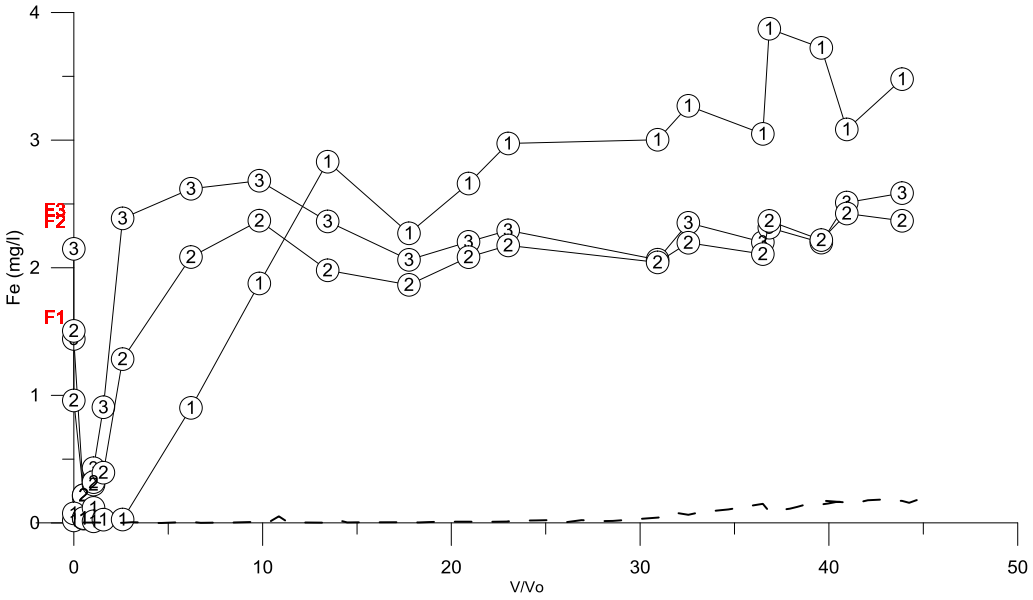

Figure 3-2 Evolution of the iron concentrations after injection of 4000 m³ of oxygenated water in well 3. The stripped line indicates the iron concentrations in the abstracted water. The evolution of the concentrations in the monitoring screens (1,2 and 3) are indicated with circles with the corresponding screen number. The concentrations measured before the start of the experiment are given at the left of fthe Y-axis labelled in red as F1, F2 or F3 depending on the screen.

Manganese

The abstracted manganese concentrations, on the other hand, increased steadily over time (Figure 3-3). During the first 20 pore volumes the abstracted manganese concentrations remained below the initially observed concentrations at the monitoring screens. From pore volume 28 onwards, the abstracted manganese concentrations were higher than the initial manganese concentration range measured in the monitoring screens.

During abstraction of the first pore volume (PV) the monitoring screens show low manganese concentrations, corresponding to a mixture of manganese-free injected water and native water. After that, the concentrations moved back to the initial concentration levels measured in the monitoring screens (marked in red in Figure 3-3 as F1, F2 and F3), and stabilized at background concentrations. Screen 1 shows somewhat a retarded behavior in reaching the background concentrations suggesting that some of the iron removal occurred already beyond this screen.

The abstracted manganese concentrations suggest that infiltration of oxygenated water results firstly in manganese removal by oxidation and precipitation as manganese oxides (MnO_x) (discussion on these reactions included in section 3.4) and in a later increase of manganese concentrations, even above the initial groundwater levels, by reduction of the oxides formed initially. This reduction is driven by the inflowing native groundwater with dissolved Fe^{2+} during continuous abstraction. This explains the additional iron removal compared to the initial theoretical efficiency and the increased manganese concentrations after a certain amount of pore volumes.

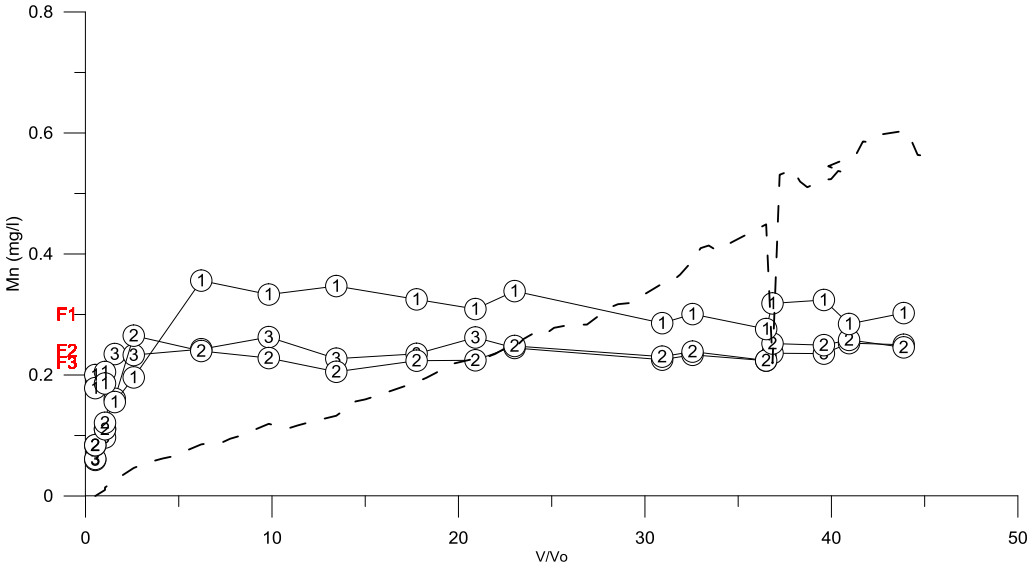

Figure 3-3 Evolution of the manganese concentrations after injection of 4000m³ of oxygenated water in well 3. The dashed line indicates the manganese concentrations in the abstracted water. The concentrations in the monitoring screens (1,2 and 3) are indicated with circles with the corresponding screen number. The concentrations measured before the start of the experiment are given at the left of the Y-axis labelled in red as F1, F2 or F3 depending on the screen.

The fact that the abstracted manganese concentrations increased over time while the monitoring screens remained constant indicates that the processes by which manganese is first oxidized and then the MnO_x precipitates are reduced, occurred within a diameter of less than 5 m away from the well.

As observed for the iron concentrations, also the arrival of manganese concentrations at background levels was delayed at screen 1 relative to screens 2 and 3, indicating, to a lesser extent, also the occurrence of manganese removal at this monitoring screen. This could be due to a higher permeability at this level causing the injected water to penetrate deeper into the aquifer or a lower reactivity of the sediment allowing the oxygen to penetrate further for iron and manganese removal. The breakthrough of chloride during injection at the different screens was used to evaluate whether there were notable differences in permeability for the different monitoring depths.

Chloride and calcium

As chloride behaves conservatively, chloride concentrations were used to assess the contribution of groundwater at the three different monitoring levels to the abstracted groundwater (Figure 3-4). The relatively stable concentrations at the monitoring wells and in the abstracted water, indicate that the abstracted water is a homogeneous mixture of the groundwater measured in the three monitoring screens. This suggests that either all the depths contribute similarly to the abstracted water or that the groundwater is drawn predominantly from the middle part of the aquifer. That the level at which the chloride concentrations stabilized in the monitoring screens differed from those determined prior to the field test (Table 3-4) is attributed to local variations in the original water quality. Similar stabilization at variable native concentration levels occurred for other elements such as

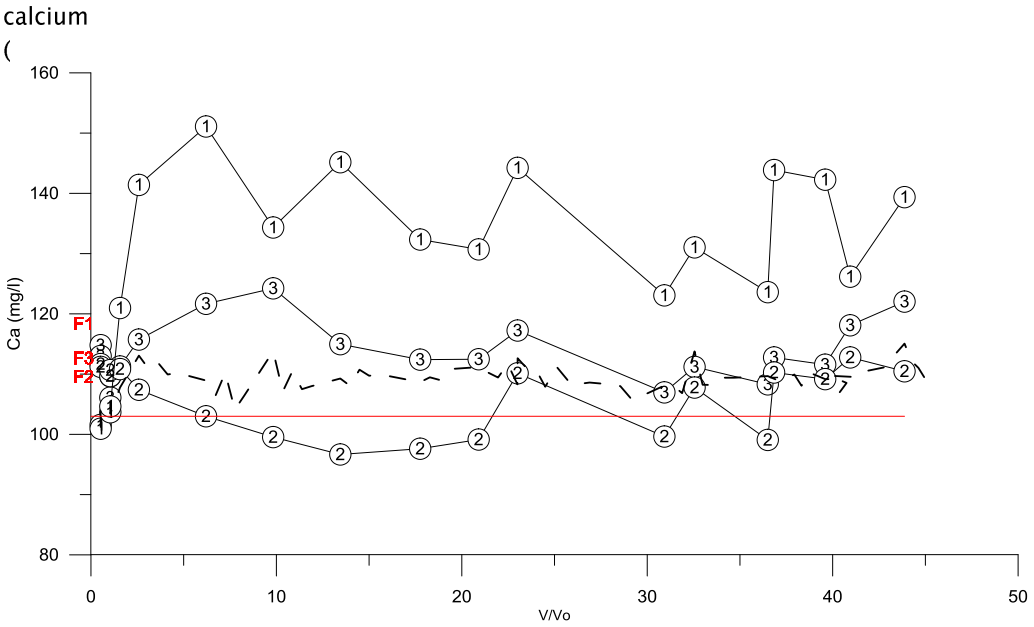

Figure 3-5). A closer look at the Cl breakthrough indicates that the injected water reaches at the same time the three monitoring screens, and that after 2.5 PV the concentrations in those screens stabilize at background values. This suggests that the permeability along the three depths is similar, and thus that a lower reactivity at the depth of monitoring screen 1 explains the observed retardation of iron and manganese concentrations at this screen during abstraction.

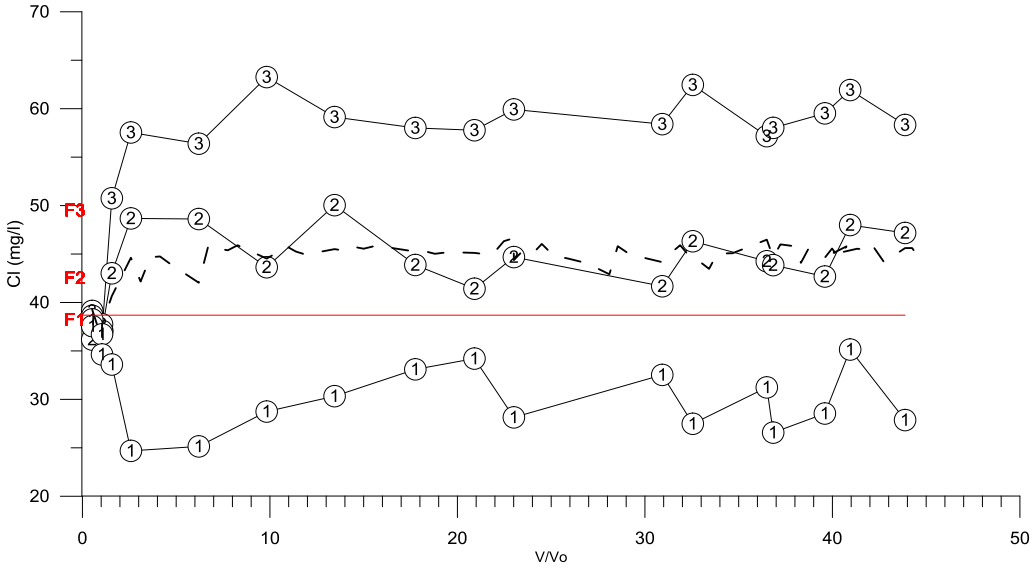

Figure 3-4 Evolution of the Chloride concentrations after injection of 4000m³ of oxygenated water in well 3. The hatched line indicates the chloride concentrations in the abstracted water. The concentrations in the monitoring screens (1,2 and 3) are indicated with circles with the corresponding screen number. The concentrations measured before the start of the experiment are given at the left of the Y-axis and labelled in red as F1, F2 or F3 depending on the screen. The averaged infiltrated concentrations are given as a red line.

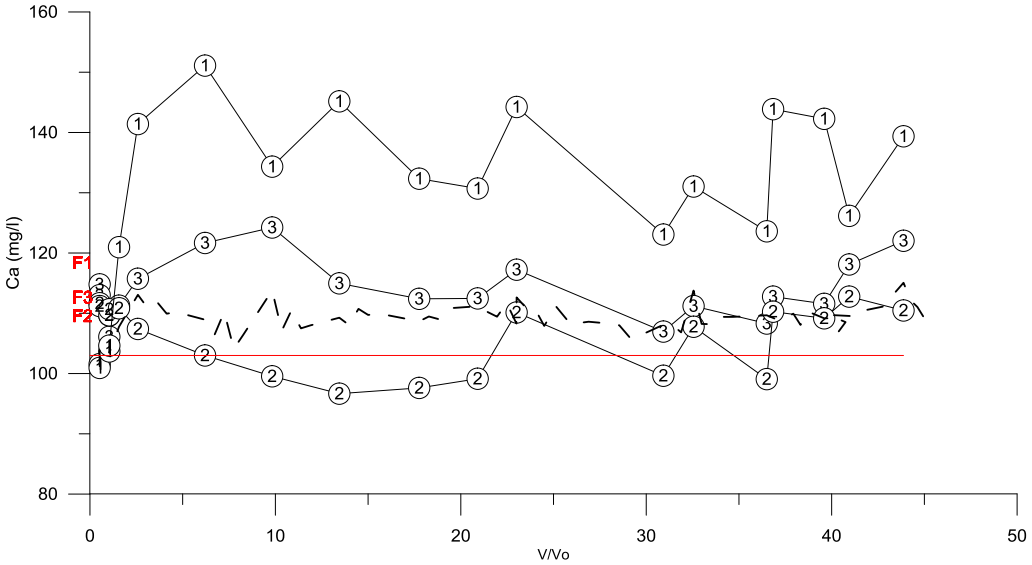

Figure 3-5 Evolution of the calcium concentrations after injection of oxygenated water in well 3. The stripped line indicates the dissolved calcium concentrations in the abstracted water. The concentrations in the monitoring screens (1,2 and 3) are indicated with circles with the corresponding screen number. The concentration measured before the start of the experiment are given at the left of the Y-axis and labelled in red as F1, F2 or F3 depending on the screen The averaged infiltrated concentrations are given as a red line.

3.3 Field pilot at well 10

The initial iron concentrations measured before the start of the experiment in the monitoring screens near well 10 ranged between 0.05 mg/l in screen 2 and 8.37 mg/l in screen 3 of the monitoring well. The manganese concentrations vary between 0.21 and 1.03 mg/l (Table 3-5) and the pH between 6.93 and 7.4. The groundwater around well 10 was fresh (EC between 63 and 86 mS/m) with Ca and HCO_3 as the main ions.

Table 3-5 Native groundwater quality in the monitoring screens beside well 10 and average of the injected water (2 samples per day).

		PB01	PB02	PB03	P10-IN	P10 -IN
Date		23-3-2015	23-3-2015	23-3-2015	23-3-2015	10-4-2015
Time		10:23:00	10:39:00	10:57:00	15:21	Average 2 days
Depth (m-surface)		26,50-27,50	33,00-34,00	39,00-40,00		
pH in situ	pH	7.4	7.01	6.93	7.34	7.35
Ca	mg/l	122.30	168.50	165.07	104.45	105.48
Cl	mg/l	37.32	49.16	47.03	40.3	40.32
DOC	mg/l	3.05	9.68	10.08		
Fe total	mg/l	0.80	0.07	8.10	<0.05	<0.05
Fe dissolved	mg/l	0.70	0.05	8.37	<0.01	<0.01
EC 20C	mS/m	63.10	78.30	85.70	58,7	57.93
HCO_3	mg/l	302.38	335.56	389.79	242,44	230.62
K	mg/l	1.92	2.43	4.96	2,68	2.55
Mg	mg/l	9.06	8.74	10.42	8,01	8.55
Mn	mg/l	0.21	1.03	0.47	<0.005	<0.005
Na	mg/l	28.16	27.31	23.25	25,6	22.96

NH_4	mg NH4 / l	0.20	1.11	0.92	<0.03	<0.03
SO_4	mg SO4 / l	76.87	131.79	146.22	87,91	86.65
Sr	µg/l	393.97	546.33	930.47	658,3	619.77
O_2	mg/l				20	20

3.3.1 Online monitoring

Continuous monitoring of O_2, pH and EC took place during abstraction of the first volumes (Cycle 1 – oxygenated water) and during the abstraction of the first volumes after permanganate injection (Cycle 2) (Figure 3-6). This allowed for comparison between the two types of infiltrated water. The oxygen front after the permanganate treatment (Figure 3-6, right) was retarded with respect to the oxygen front during cycle 1 (Figure 3-6, right). This suggests that part of the permanganate lowered the reactivity of the sediment for oxygen.

While the pH and the EC in the abstracted water go slightly down and up, respectively, in the first cycle, the permanganate treatment resulted in stronger increases of both pH and EC. The observed increase in pH (Fig. 3-6) is attributed to the proton consuming reaction of the permanganate with sedimentary organic matter in the aquifer. This increase is only partly compensated by the production of CO_2 that is released from this reaction (Eq 3.2.1):

MnO_4 oxidizing SOM: $3CH_2O + 4MnO_4^- + 4H^+ \rightarrow 3CO_2 + 4\ MnO_2 + 5H_2O$ (Eq 3.2.1)

The peak of EC is the result of the increased ionic strength of the infiltrated water with sodium permanganate solution.

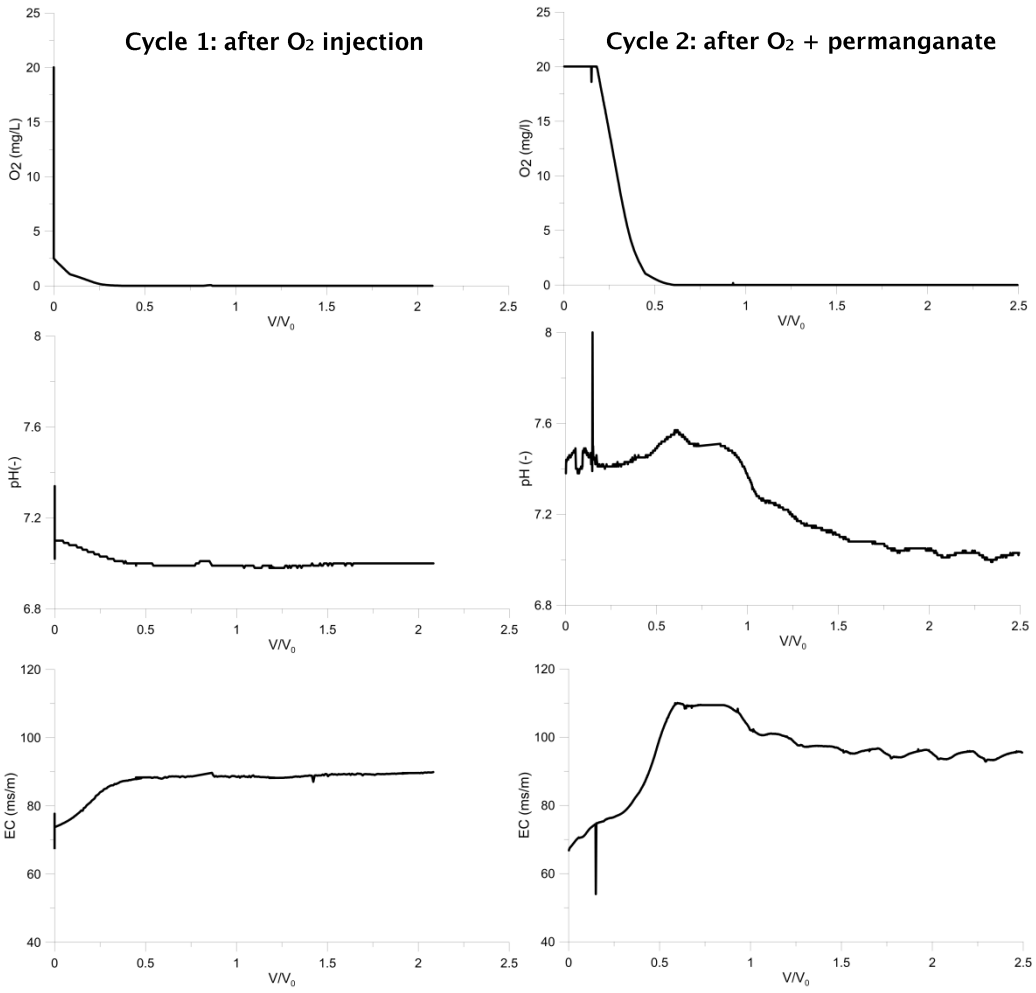

Figure 3-6 Continuous monitoring of O_2, pH and EC after a cycle of SIR with infiltration of oxygenated water (left column) and after a cycle with infiltration of permanganate solution (right column).

3.3.2 Observed iron and manganese concentrations

Iron

The iron concentrations measured in the monitoring screens varied along with the injection and recovery cycles (Figure 3-7), meanwhile the iron concentrations in the abstracted water remained low.

After infiltration of water enriched with oxygen (cycle 1) the iron concentrations in the monitoring well screens dropped as a result of the infiltrated iron-free water. After some hours of abstraction the iron concentrations measured in the screens stabilized at native concentrations. The abstracted water remained iron-free. The differences between the

measured iron concentrations at the monitoring well and the concentrations at the abstraction well indicate that most of the iron removal processes occur within 5m from the pumping well. While the monitoring well showed stable native values, the abstraction well still showed iron concentrations close to the detection limits.

Immediately after permanganate infiltration, low iron concentration values are observed again in the screens of the monitoring wells as a result of the infiltrated water. Thereafter the iron concentrations in screen 3 increased, while those of screens 1 and 2 remained low until approximately 10 PV, after which the dissolved iron concentrations moved back to their native levels. The iron concentrations in screen 3 of the monitoring well reached values of 10.22 mg/l, slightly higher than the initial value..

After a third cycle of injection of oxygenated water, the abstracted iron concentrations remained low, with values under the 0.2mg/l for the first 11 PV. The concentrations measured in screen 3 increased again to values above the initial values. Screen 1 showed concentrations similar to the initial values. At screen 2 iron concentrations started to increase after the 23rd PV, along with increased abstracted iron concentrations.

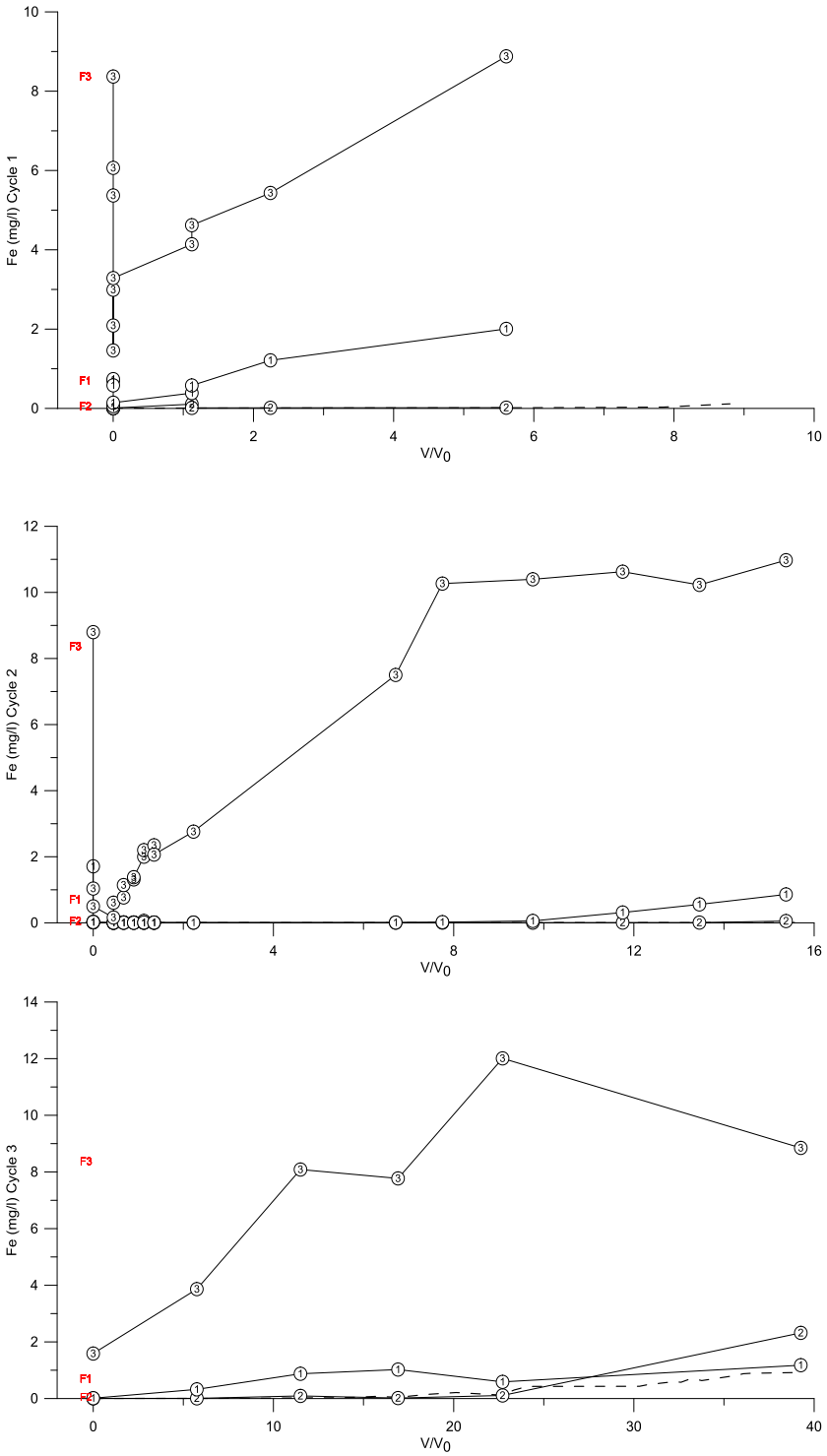

Figure 3-7 Evolution of the iron concentrations after injection of (Cycle 1) oxygenated water, (Cycle 2) permanganate solution with oxygenated water, and (Cycle 3) oxygenated water in well 10. The stripped black line indicates the iron concentrations in the abstracted water. The concentrations in the monitoring screens (1, 2 and 3) are indicated with circles with the corresponding screen number. The concentrations measured before the start of the experiment are labelled in red as F1, F2 or F3 depending on the screen.

Manganese

The native manganese concentrations observed in the monitoring screens (<0,5 mg/L) were similar to the abstracted concentrations and remained so after the first infiltration cycle with oxygen-rich water (Figure 3-8).

Immediately after infiltrating water enriched with permanganate (129 mg $NaMnO_4$/l) there was a peak in the total manganese concentrations (including permanganate) in all the monitoring well screens (Figure 3-8), above all in screen two, where concentrations reached up to almost 320 mg/l. The simultaneous breakthrough of sodium concentrations at the different screens indicates that the permeability at the monitoring levels is similar. The higher Mn concentrations at screen 2 therefore indicate that permanganate has been able to infiltrate deeper into the aquifer due to a lower sediment reactivity at this screen depth. This resulted in precipitation of manganese oxides beyond screen 2 which, in turn, can be reduced by incoming Fe resulting in an increase of the Mn concentrations during abstraction. This explanation is in keeping with the delayed rise of iron concentrations at screen 2 in comparison with screens 1 and 3 (Figure 3-7).

After less than one month of abstraction (8 PV), the abstracted water showed a peak of 8.8 mg Mn/l. The concentrations measured in monitoring screen 2, were similar to those measured in the abstracted water, which decreased after the 8.8 mg/l peak. Screens 1 and 3 showed low concentrations during most part of this cycle. This is in keeping larger amounts of manganese oxides precipitated upstream of monitoring screen 2, resulting in mobilization of manganese due to reduction by inflowing Fe(II) with the native groundwater monitoring.

The third cycle involving oxygen-rich water infiltration, decreased initially the abstracted manganese concentrations but after some hours the Mn concentrations started increasing slowly again reaching after 23 PV concentrations up to 7.37 mg/l. After that peak the concentrations started decreasing until abstraction was ended after 40 PV (100 days). Screen 2 showed increased concentrations relative to those of native groundwater during the whole cycle. The manganese concentrations measured in screens 1and 3 were similar to the native ones during abstraction.

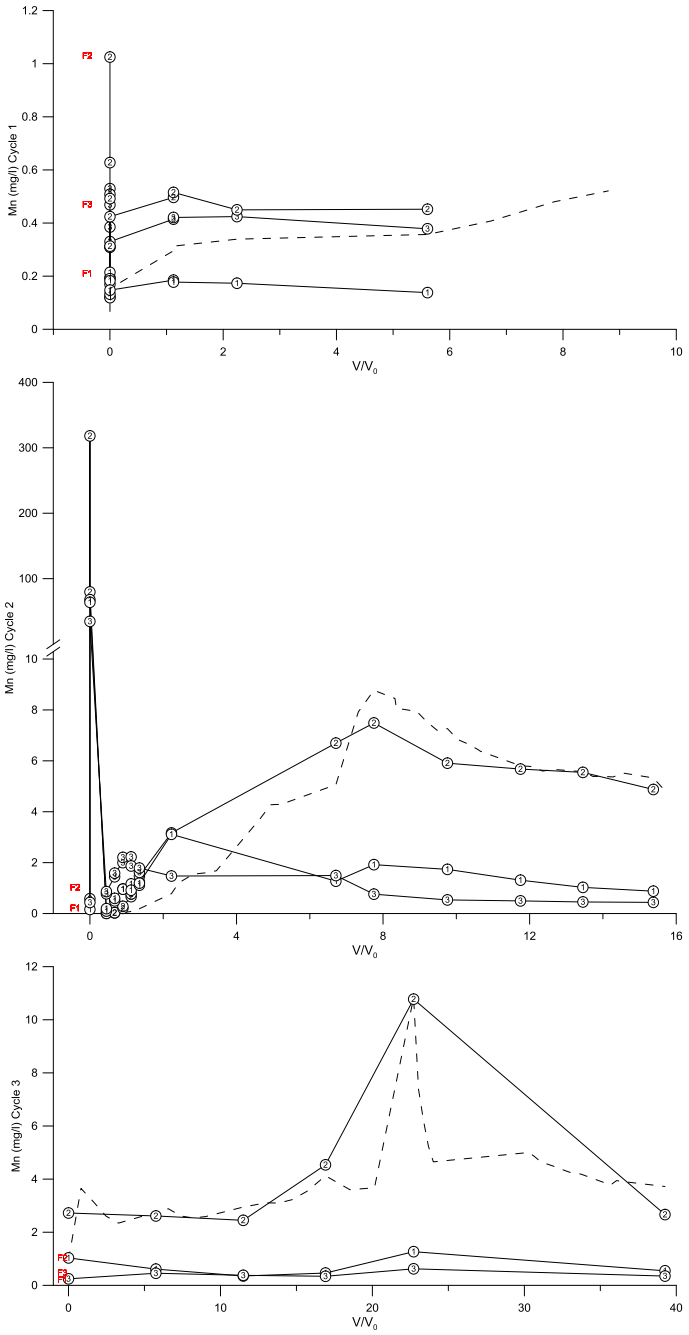

Figure 3-8 Evolution of the manganese concentrations after injection of successively (1) oxygenated water (2) permanganate solution with oxygenated water, and (3) oxygenated water in well 10. The stripped line indicates the manganese concentrations in the abstracted water. The concentrations in the monitoring screens (1,2 and 3) are indicated with circles with the corresponding screen number. The concentrations measured before the start of the experiment are labelled in red as F1, F2 or F3 depending on the screen.

Chloride

During the field pilot at well 10, the abstracted chloride concentrations in the monitoring wells and the abstracted water remained fairly stable during the three abstraction phases (Figure 3-9). The monitoring well shows Cl concentrations in screen one that decreased with respect to the initial concentrations (~40 mg/l) after abstraction meanwhile screen two and

three increase their Cl concentrations. After infiltration of water with permanganate (cycle 2) screen 1 and 2 increased and decreased their concentrations respectively towards their native values (around 37 and 49 mg/l), and screen 3 continued increasing. After the third cycle where oxygenated water is injected, screen 3 showed elevated Cl values and screen 1 and 2 values similar to the native ones. Possibly the continuous abstraction resulted in arrival of deeper waters with a higher chloride content towards the deepest monitoring screen 3, from below a discontinuous clay layer. However this did not affect the overall abstracted chloride concentration. During infiltration Cl breaks through simultaneously at the three screens, confirming the similar permeability at these monitoring wells as already inferred from the breakthrough of sodium with the injection of sodium permanganate in cycle 2.

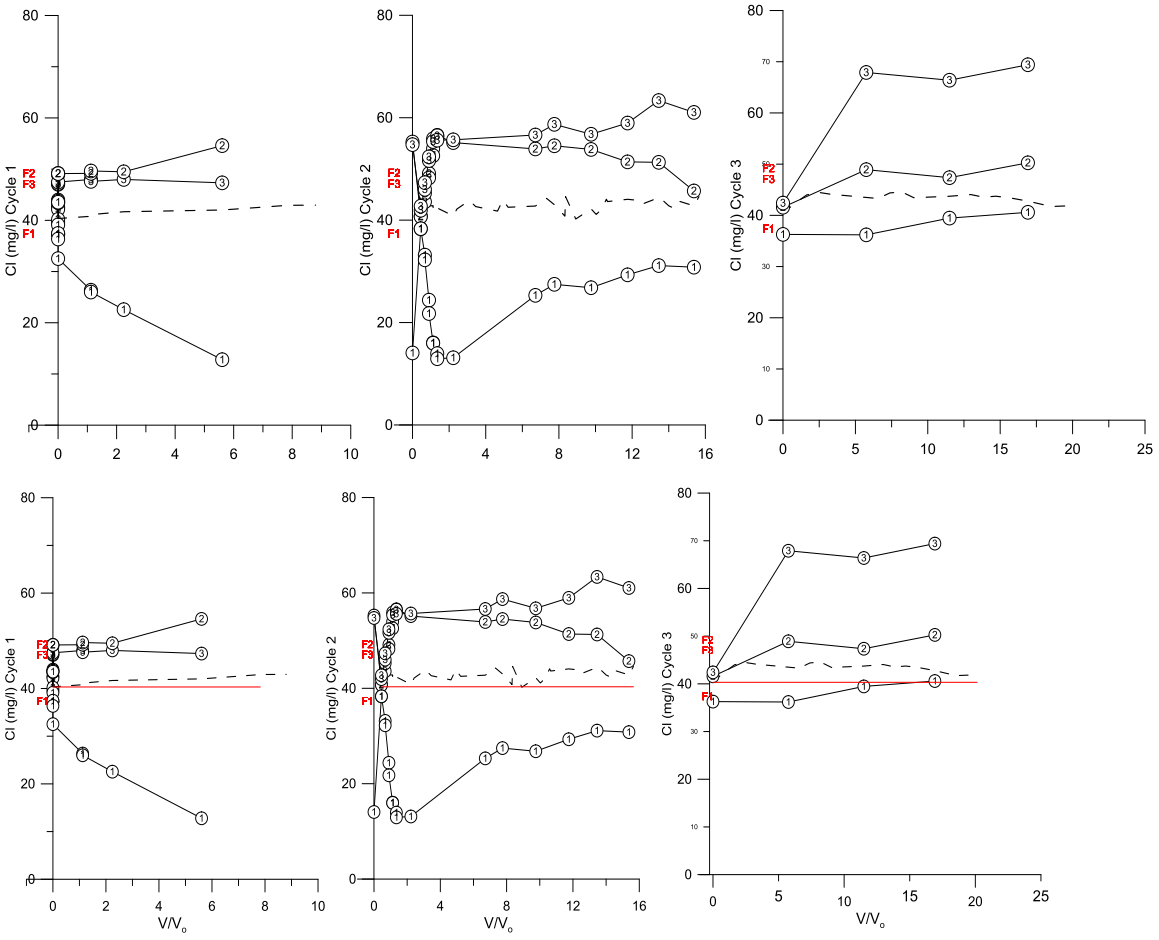

Figure 3-9 Evolution of the chloride concentrations after successive injection of (1) oxygenated water (2) permanganate solution with oxygenated water and (3) oxygenated water in well 10. The stripped line indicates the chloride concentrations in the abstracted water. The concentrations in the monitoring screens (1,2 and 3) are indicated with circles with the corresponding screen number. The concentrations measured before the start of the experiment are given at the left of the Y-axis and labelled in red as F1, F2 or F3 depending on the screen.

Sulfate

The slight increases of sulfate concentrations observed in the abstracted water (Figure 3-10) in well 10 suggests limited pyrite oxidation during cycle 1, which fits with the sediment composition (Table 3-2). After the permanganate treatment, the abstracted sulfate concentrations decrease slowly and during cycle three they remained constant, which suggests that the permanganate treatment reduced the overall reactivity by pyrite. Similarly for the monitoring screens (Figure 3-10), the observed sulfate concentrations at screen 1 increase slightly with respect to the initial native values, which could be due to pyrite oxidation (from 80 to 90 or 100 mg/l) after cycle 1 and 2 and remains constant after cycle 3 at around 92 mg/l.

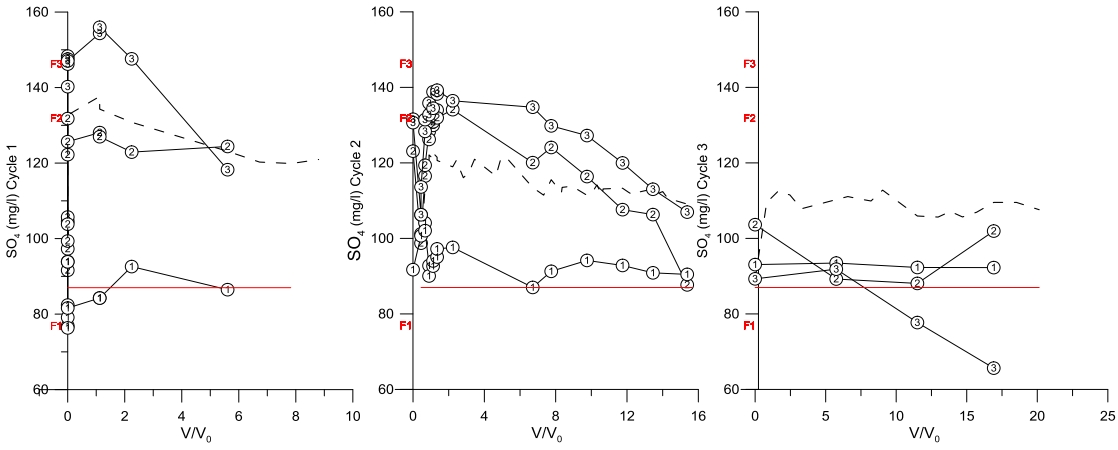

Figure 3-10 Evolution of the sulfate concentrations after injection of (1) oxygenated water (2) permanganate solution with oxygenated water and (3) oxygenated water in well 10. The stripped line indicates the sulfate concentrations in the abstracted water. The concentrations in the monitoring screens (1,2 and 3) are indicated with circles with the corresponding screen number. The concentrations measured before the start of the experiment are given at the left of the Y-axis and labelled in red as F1, F2 or F3 depending on the screen. The average infiltrated concentration is marked as a red line.

DOC

The dissolved organic carbon concentrations (*Figure 3-11*) indicate that the oxidation of sedimentary organic matter by permanganate also resulted in increased concentrations of dissolved organic matter. This confirms that the permanganate acted to reduce the background reactivity by both oxidation and mobilization of organic matter.

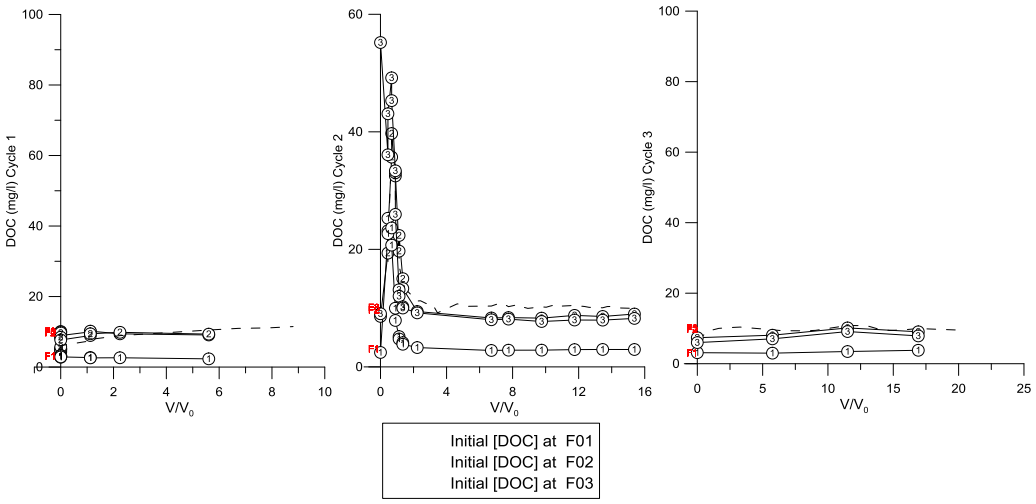

Figure 3-11 Evolution of the DOC concentrations (mg/l) after injection of (1) oxygenated water (2) permanganate solution with oxygenated water and (3) oxygenated water in well 10. The stripped line indicates the DOC concentrations in the abstracted water. The concentrations in the monitoring screens (1,2 and 3) are indicated with circles with the corresponding screen number. The concentrations measured before the start of the experiment are given at the left of the Y-axis and labelled in red as F1, F2 or F3 depending on the screen.

3.4 Controls on iron and manganese concentrations

According to the iron concentrations in the native groundwater in the monitoring screens at well 3 (2mg/l) and the injected water rich in oxygen (20 mg/l) there is maximum potential for SIR efficiency of around 69 at that well. This is based on the 4/1 stoichiometric relationship for the oxidation of iron by oxygen (Eq 3.1), whether oxidation of ferrous iron occurs homogenously or heterogeneously adsorbed to iron hydroxides (reaction equations 3.4a to 3.4c). Iron hydroxides form in contact with oxygen and the rate of further iron adsorption is highly dependent on pH (Eq 3.4a to Eq 3.4c).

The wide range in iron concentrations measured in the monitoring screens at well 10 indicate that very different iron removal efficiencies can be achieved at various depths. For sediments with groundwater with low iron concentrations oxidative removal of background reactivity gives a high potential for the increase of the removal efficiency. Whereas the potential is lowest for aquifers with high iron concentrations in the native groundwater. The fact that screen 3 shows high iron concentrations will mean that the possible improvement in efficiency is highly limited and the iron breakthrough will happen sooner.

The analysis on the sediment samples in both wells leads to thinking that there is presence of organic matter (CH_2O) , which will react with oxygen to form CO_2 (5, and section 3.2.2) and therefore will compete for oxygen with the iron, resulting in a lowering of the iron removal efficiency. The same applies for the oxidation of pyrite, which is expected to decrease the iron removal efficiency.

$$4Fe^{2+} + O_2 + 10H_2O \rightarrow 4Fe(OH)_3 + 8H^+ \qquad log\,k = 32.159 \qquad (3.1)$$

$$Ca^{2+} + Fe - X_2 = Ca - X_2 + Fe^{2+} \qquad log\,k = -0.44 \qquad (3.2)$$

$$4Fe(OH)_2OFe^+ + O_2 + 10H_2O = 8Fe(OH)_3 + 4H^+ \qquad log\,k = 4.3 \qquad (3.3)$$

$$*Hfo_w - OH + Fe^{2+} = Hfo_w - OFe^{+} + H^{+} \qquad log(K) = -2.98 \qquad (3.4a)$$

$$Hfo_w - OH + Fe^{2+} + H_2O = Hfo_w - OFeOH + 2H^{+} \qquad log(K) = -11.55 \qquad (3.4b)$$

$$Hfo_s - OH + Fe^{2+} = Hfo_s - OFe^{+} + H^{+} \qquad log(K) = -0.95 \qquad (3.4c)$$

**The chemical binding to the surface of ferrihydrite is, according to the two layer model of Dzombak and Morel (1990), distributed among weak affinity (Hfo_w) and strong affinity (Hfo_s) sites, which exist in a proportion of 0.2 and 0.005 mol sites / mol ferrihydrite, respectively. A broad range in surface area of ferrihydrite has been reported to in literature. Equation 3.1 from (Appelo et al., 1999) and Equation 3.4a from (Appelo and Vet, 2003)*

$$4CH_2O + H_2O = CO_2 + 4H^{+} + 4e^{-} \qquad log\,k = 0.8 \qquad (3.5)$$

Dissolved manganese concentrations are also expected to be reduced by the injection of oxygen-rich water due to the formation of manganese oxides (Eq 3.6 and Eq 3.7) and to the sorption to the hydroxides (Eq 3.8 and Eq 3.9). However, with regard to the original native manganese concentrations, a net increase in concentrations has been observed in the abstracted water in the end of the abstraction at well 03. This can result from the combined effect of reduction of MnO_2 by Fe(II) followed by the preferential sorption of iron on hydroxides and cation exchangers (Eq 3.8) over manganese. But the main contribution is expected to be due to reduction of manganese oxides by iron, after oxidation of the dissolved manganese into manganese oxides. As a result iron concentrations decrease and dissolved manganese concentrations increase (Eq 3.10).

$$Mn^{2+} + \frac{1}{2}O_2 + 2H^{+} \rightarrow Mn^{4+} + H_2O \qquad log\,K = 27.36 \qquad (3.6)$$

$$Mn^{4+} + 2H_2O \rightarrow MnO_2 \downarrow + 4H^{+} \qquad log\,K = 3.78 \qquad (3.7)$$

$$Fe^{2+} + Mn - X_2 = Fe - X_2 + Mn^{2+} \qquad log\,k = 0.91 \qquad (3.8)$$

$$Hfo_w - OH + Mn^{2+} = Hfo_w - OMn^{+} + H^{+} \qquad log(K) = -3.5 \qquad (3.9a)$$

$$Hfo_s - OH + Mn^{2+} = Hfo_s - OMn^{+} + H^{+} \qquad log(K) = -0.4 \qquad (3.9b)$$

$$2Fe^{2+} + MnO_2 + 4H_2O \rightarrow 2Fe(OH)_3 + Mn^{2+} + 2H^{+} \qquad (Eq\ 3.10)$$

The presence of calcite in the system, confirmed for well 10 by the presence of shell fragments, supports pH-buffering processes. Subsequent to whether oxidation reactions produce or consume protons, they will result in dissolution or precipitation of calcite and an increase or decrease of calcium concentrations in the groundwater, respectively (Eq 3.11, Eq.3.12).

Proton -buffering:

$$2H^{+} + CaCO_3 \rightarrow Ca^{2+} + CO_2 + H_2O \qquad log\ k = 9.74 \qquad (3.11)$$

Following CO_2 production

$$CO_2 + CaCO_3 + H_2O \rightarrow Ca^{2+} + 2HCO_3^{-} \qquad log\ k = -6 \qquad (3.12)$$

Most of the analyses for well 10 plot on the calcite equilibrium line under varying CO_2 pressures (red line in Figure 3-12), indicating that calcite is acting as the main pH buffer. In Well 03, however, the Ca and HCO_3 concentrations respond mainly to the release of protons by the oxidation of iron by O_2. In contrast, the samples taken in well 10 after permanganate dosing reflect the proton consumption due to oxidation of organic matter by the permanganate (towards higher alkalinity and lower calcium relative to the CaCO3-CO2 equilibrium line).

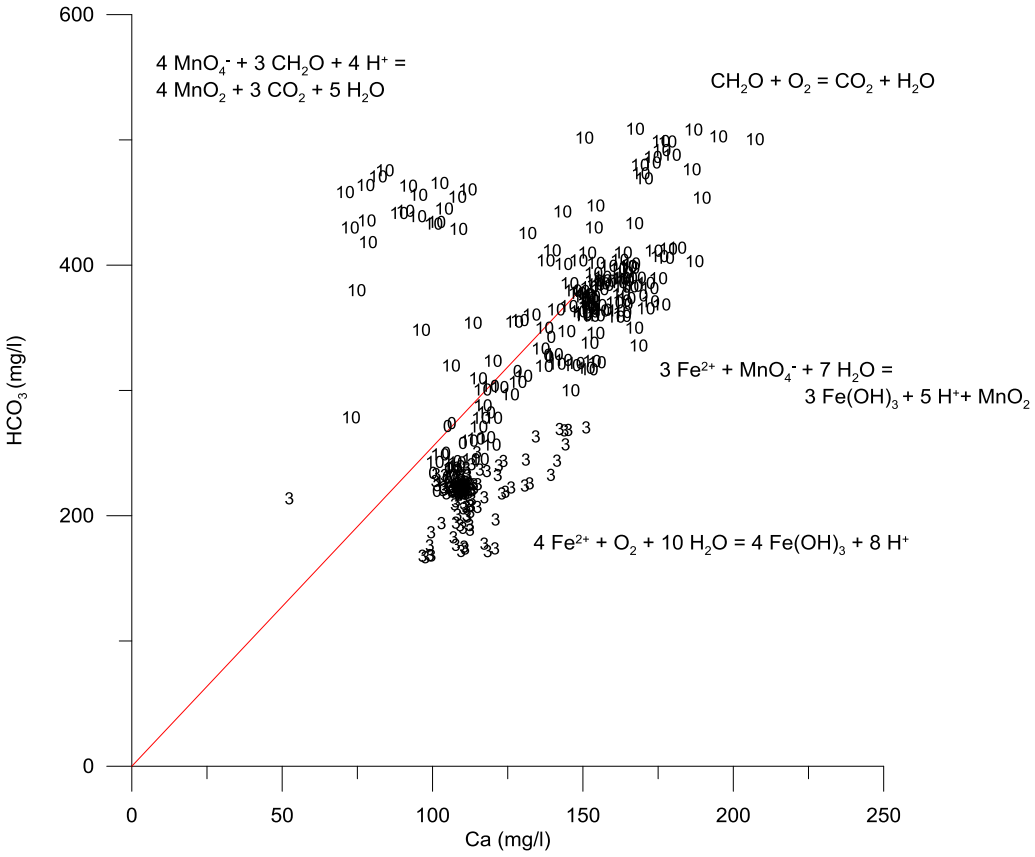

Figure 3-12 Ca^{2+} versus $HCO3^-$ in the water recovered from the SIR wells 3 and 10. The red line represents calcite equilibrium for increasing CO_2 pressure.

The treatment of the aquifer sediment with the addition of permanganate to the injected water resulted, in addition to the reactions described above, in the reactions listed below .

MnO_4 oxidizing SOM (reduction of the background reactivity)

$$3CH_2O + 4MnO_4^- + 4H^+ \rightarrow 3CO_2 + 4\ MnO_2 + 5H_2O \quad \text{(Eq. 3.12)}$$

MnO_4 oxidizing Fe(II) (removal of iron)

$$3Fe^{2+} + MnO_4^- + 7H_2O \rightarrow 3Fe(OH)_3 + MnO_2 + 5H^+ \quad \text{(Eq 3.13)}$$

MnO_4 oxidizing Mn(II) (removal of manganese)

$$3Mn^{2+} + 2MnO_4^- + 2H_2O \rightarrow 5MnO_2 + 5H^+ \qquad \text{(Eq 3.14)}$$

MnO_4 oxidizing pyrite (reduction of the background reactivity)

$$FeS_2 + 5\ MnO_4^- + H^+ \rightarrow 5MnO_2 + 2SO_4^{2-} + 5H_2O \qquad \text{(Eq 3.16)}$$

In addition to these redox reactions, the abstracted concentrations of iron and manganese are also influenced by mixing with the native groundwater. Therefore, some of the samples from well 10 and well 3 plot on the Mn:Fe ratio for native groundwater of about 1:16 (*Figure 3-13*). Most of the samples for well 10 plot have elevated Mn concentrations (one order of magnitude higher than the standard native Mn concentrations) with very low iron concentrations and therefore plot along the Y-axis and illustrate the mutually excluding effect caused by the reduction of manganese oxides by Fe^{2+} resulting in the mobilization of Mn^{2+} and immobilization of Fe in hydroxides (equation 13).

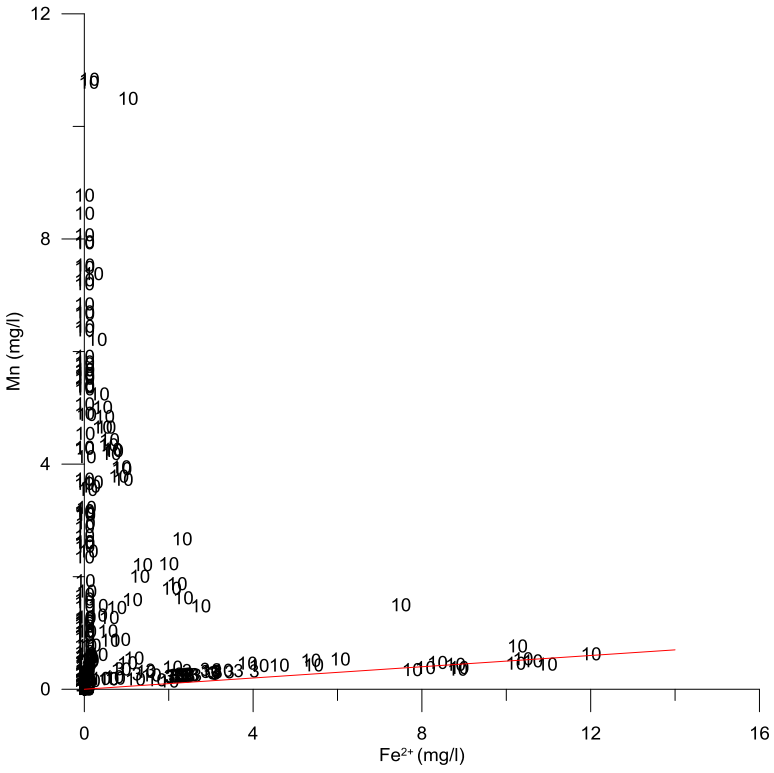

Figure 3-13 Fe^{2+} versus Mn in the water recovered from the SIR wells 3 and 10. The red line represents the mixing line with the groundwater and the upper part of the measurements indicate the Iron and Manganese concentrations expected from iron reducing manganese-oxides.

3.5 Fate and impact of permanganate application

3.5.1 Impact of permanganate application on abstracted groundwater

The addition of permanganate in the infiltrated water resulted in purple-colored water that could be used as a visual tracer for its transport to the monitoring wells. During abstraction at the well, all infiltrated permanganate had been consumed during sediment passage, as illustrated by the lack of any remaining coloration.

The presence of permanganate triggered several reactions (described in section 3.4) that modified the composition of the abstracted groundwater, like mobilization of DOC (Figure 3-11) or the precipitation of calcite with buffering purposes, which resulted in higher HCO_3 concentrations.

In addition to these effects on the major chemistry, attention was paid to trace elements. These can either be present in the injected permanganate solution or be mobilized by interaction with the sediment. Although the trace element concentrations of the permanganate type used (Carusol C, certified for potable water production) could not be determined, a certain amount of trace elements was assumed to be present. Since those elements are likely similar to those in other sodium permanganate solutions, the elements reported for a 40% sodium permanganate solution used in soil remediation (RemOx, .Table 3-6) were used for comparison. .The observed concentration peaks in the abstracted water relative to background for Cr, Se and to a lesser extent Cu are therefore thought to result from the infiltrated permanganate solution. The evolution of Ba, Pb, and Ni (Figure 3-14) is less evident, likely in part by the retardation that these elements undergo due to adsorption to sediment phases. Therefore the highest Ba concentrations in monitoring screen 3 could be explained as displacement by the relatively high inflowing iron concentrations for this monitoring screen (Fig.3-7). Possibly part of the increase in Ni concentrations is due to pyrite oxidation. Following the peaks for some of these elements, the concentrations in the abstracted water returned to background levels within 3 abstracted pore volumes. Apart from the slight exceedance observed in the monitoring screens during injection for Cr, the concentrations for these elements remained below their respective drinking water standards (Cr<50 µg/L, Cu <2000 µg/L, Se <10 µg/L, Pb<10 µg/L, Ni<20 µg/L , and for Ba there is no reference value given in the law of 1998 however in the previous European law of 1993 the standard value for Ba was 300 µg/L) in both the monitoring screens and the abstracted groundwater during the field experiment.

Table 3-6 The 40% sodium permanganate type infiltrated in this study was Carusol-C. For comparison the trace element composition of the 40% sodium permanganate solution type manufactured for soil remediation (RemOx) is shown. Source: Carus Chemical Company.

Element	Typical Analysis (mg/kg)	Specifications (mg/kg)	DL* (mg/kg)	Element	Typical Analysis (mg/kg)	Specifications (mg/kg)	DL* (mg/kg)
Ag	BDL	0.15	0.034	Fe	BDL	2.00	0.053
Al	BDL	2.00	0.24	Hg	BDL	0.03	0.003
As	BDL	4.00	0.006	Ni	BDL	0.1	0.03
Ba	2.96	15.00	0.016	Pb	BDL	0.70	0.16
Be	BDL	0.50	0.08	Sb	BDL	0.70	0.16
Cd	BDL	0.10	0.016	Se	0.0034	0.50	0.0003
Cr	3.2	5.00	0.031	Tl	BDL	3.50	0.80
Cu	BDL	0.10	0.022	Zn	0.034	0.40	0.011

DL* is detection limit
BDL is below detection limit

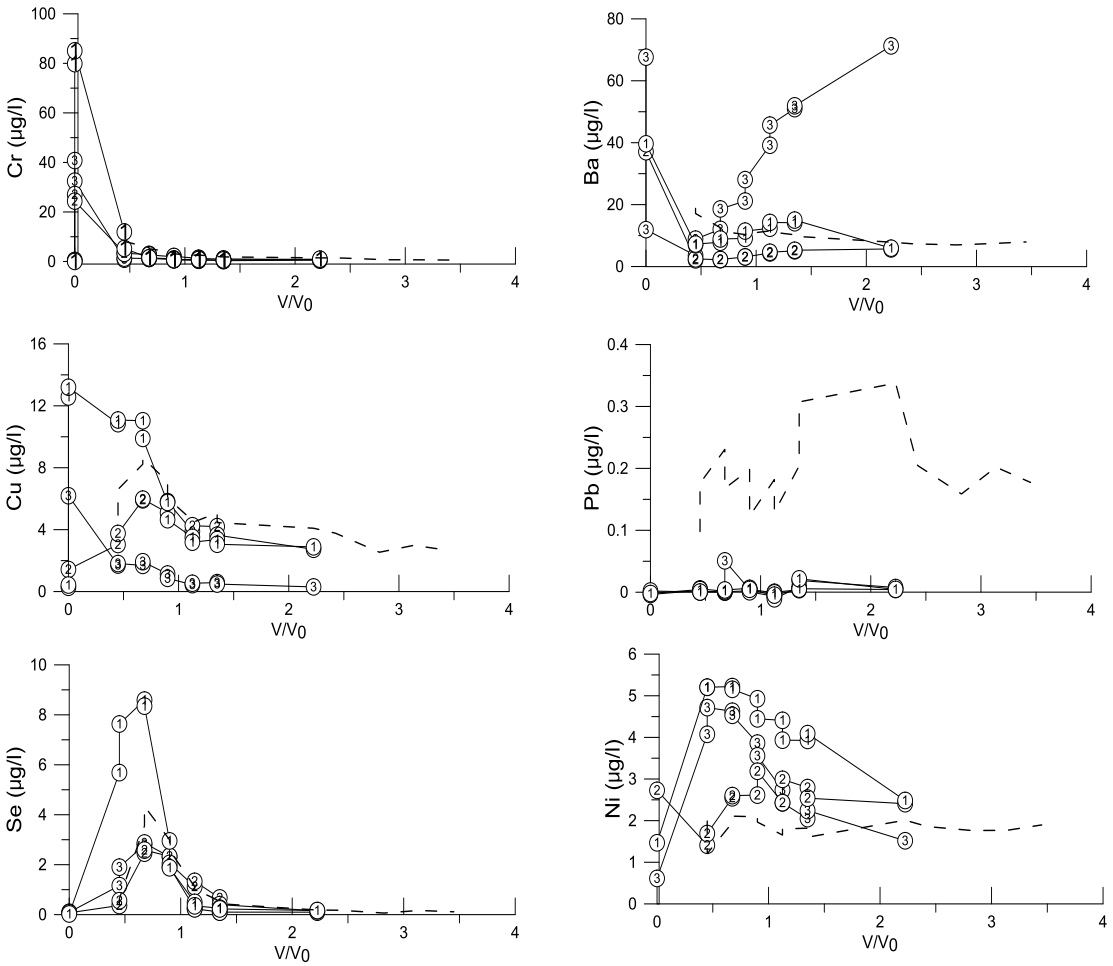

Figure 3-14 Evolution of the Cr, Cu, Se, Ba, Pb and Ni concentrations after injection of (1) oxygenated water (2) permanganate solution with oxygenated water and (3) oxygenated water in well 10. The stripped line indicates the concentrations in the abstracted water. The concentrations in the monitoring screens (1,2 and 3) are indicated with circles with the corresponding screen number.

3.5.2 Impact of permanganate application on aquifer sediment

As mentioned in the previous paragraph, one of the considerations for the interaction of permanganate with aquifer sediment was the potential resolubilization of metals and trace elements like Cr(VI). However, based on the comparison of elemental XRF analysis of sediment before and after treatment with permanganate in a batch experiment, no consistent differences indicating mobilization or immobilization of Cr could be observed after the treatment with $KMnO_4$ (Figure 3-15), except for a clear increase of Mn due to the precipitation of manganese oxides and the decrease of carbon (C) due to the oxidation of organic matter.

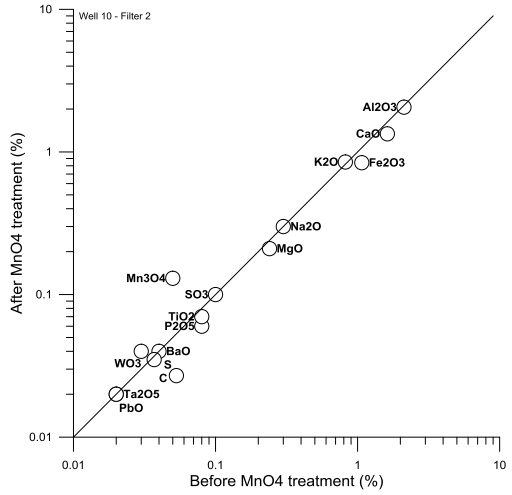

Figure 3-15 Elemental analysis by CNS analyser and XRF of aquifer sediment before and after permanganate treatment.

3.6 Removal Efficiencies during Subsurface Iron Removal

3.6.1 Observed removal efficiencies during and after field pilots

During the experiments the usual removal efficiencies (V/Vo) were surpassed until higher concentration values for the iron and Mn were recovered as part of the experiment (Table 3-7), to study their development. The efficiencies of the SIR wells 03 and 10 after the experiments have increased significantly with abstracted iron concentrations below 0.2 mg/l, as removal efficiencies one year later indicate (Table 3-8).

According to the native iron concentrations and the stoichiometry, the theoretical removal efficiency at well 3 is 69 (taking 2 mg Fe/l as native iron concentration), however, the efficiency with which the well was operated until now was 23 (on average). During the experiment at well 03, enlarging the infiltrating volume was expected to decrease the efficiency due to the fact that the recovered water would have to go through newly formed iron hydroxides with smaller sorption surface than the ones resulting from decades of operation. The efficiency, however, seemed to increase during (Table 3-7) and after (Table 3-8) the experiment, allowing for much larger abstraction volumes with low iron concentrations. This indicates a prior suboptimal iron removal efficiency was used for this well. This year the well has even shown to reach removal efficiencies of around 40.

The treatment with permanganate was thought for the well with the worst performance of the well field, with an average removal efficiency of 9. For this well, however, the potential removal efficiency changes with depth since the iron concentration varies strongly as well: 119 at 26.5 m deep (1.17 mg Fe/l), 60 at 33.5 m deep (2.31 mg Fe/l) and 16 at 40m deep

(8.84 mg Fe/l), based on the iron concentrations at the monitoring screens at the end of cycle 3. That is; with higher iron concentrations, lower potential subsurface iron removal efficiency and lower potential increase in efficiency with possible operational changes or treatments. The fact that the deepest layer of the well showed such high iron concentrations resulted in a general faster iron breakthrough, limiting the maximum efficiency that could be achieved for the well overall. Furthermore, the different background reactivity in depth, as shown by the observed manganese concentrations, contributes to making the removal efficiency strongly depth-dependent. Despite this, the treatment with permanganate did help reducing the background reactivity of the aquifer and resulted in an increase of the removal values that went from 9 to currently 11.

Table 3-7 Removal efficiencies (V/Vo), volumes and Iron and manganese concentrations during each experimental cycle.

Well	Treatment	Start date	End date	V/Vo	Fe (mg/l)	Mn (mg/l)
3	Oxygenated (with O2)	2-3-2015	3-3-2015			
		4-3-2015	2-7-2015	45.0	0.2	0.56
3	Oxygenated (with O2)	2-7-2015	2-7-2015			
		2-7-2015	9-9-2015	23.5	0.1	
10	Oxygenated (with O2)	23-3-2015	24-3-2015			
		25-3-2015	2-4-2015	8.8	0.1	0.52
10	Permanganate (with O2)	9-4-2015	11-4-2015			
		13-4-2015	9-6-2015	1.49	0.01	4.9
10	Oxygenated (with O2)	9-6-2015	9-6-2015			
		15-6-2015	24-9-2015	39.26	0.92	3.72
10	Oxygenated (with O2)	24-9-2015	24-9-2015			
		24-9-2015	6-10-2016	8.32	0.33	1.48
10	Oxygenated (with O2)	6-10-2016	6-10-2016			
		6-10-2016	16-10-2016	7.15	0.08	1.27

Table 3-8 Removal efficiencies (V/Vo), abstracted volumes and Iron and manganese concentrations one year after the experimental treatments. These values correspond to infiltrated volumes of 2000m^3

Well	Abstracted (m^3)	Date	V/Vo	Fe	Mn
3	75270	28-4-2016	37.6	<0.01	0.05
3	81900	2-5-2016	41.0	-	-
3	82790	9-5-2016	41.4	0.11	0.26
3	10000	17-5-2016	5.0	<0.01	0.06
10	22550	28-4-2016	11.3	-	-
10	14860	9-5-2016	7.4	0.13	0.24
10	21800	17-5-2016	10.9	0.20	0.47

3.6.2 Implications for optimization of SIR efficiencies

As SIR efficiency is expected to increase with time, SIR plants may at some point be operated at a suboptimal efficiency. An experiment such as the one performed here allows for aquifer characterization and field-determination of maximum recovery potentials, so that the operational parameters can be adjusted to optimize the process.

Increased ammonium concentrations due to increasing the abstracted volumes, did not seem to be a risk, background native ammonium concentrations were reached already shortly after abstraction started and stayed stable even during prolonged abstraction

(

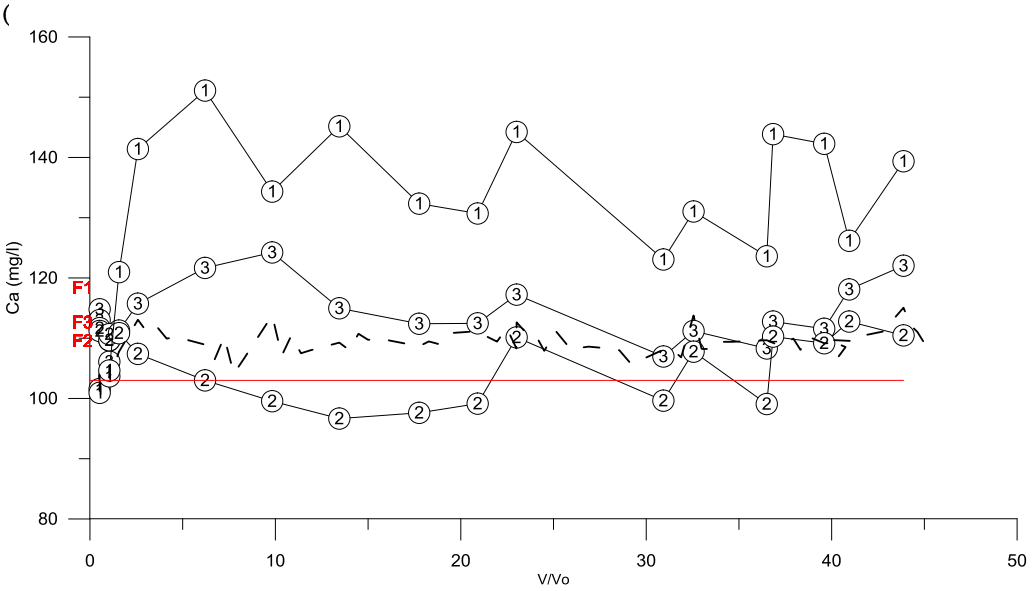

Figure 3-5). The abstracted water has somewhat higher NH_4 concentrations than those measured in the observation filters. This could likely be due to the vertically variable inflowing groundwater composition with locally higher ammonium concentrations. l.

Only a certain increase in the manganese concentrations seems to happen until iron breaks through, such as described with Figure 3-2 in section3.2.2; the initial removal of manganese from abstracted water is later compensated by abstracted concentrations higher than the background groundwater concentrations. This suggests that that there is no net removal of manganese when the abstracted volumes are based on the occurrence of iron breakthrough, only when the injection/abstraction cycle is restarted before that moment.

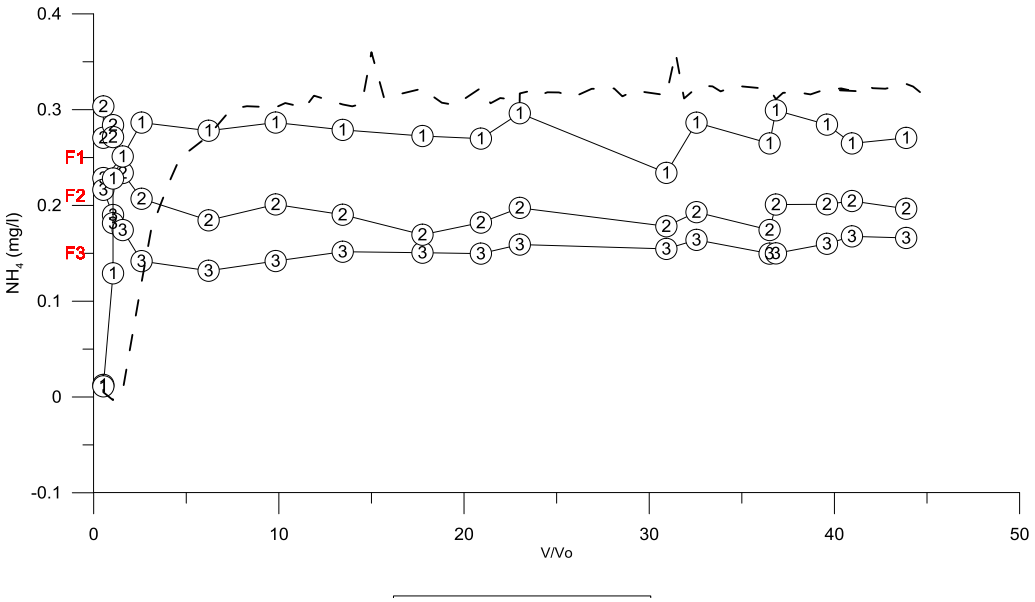

Figure 3-16 Evolution of the NH_4 concentrations after injection of oxygenated water in well 3. The stripped line indicates the dissolved NH_4 concentrations in the abstracted water. The concentrations in the monitoring screens (1,2 and 3) are indicated with circles with the corresponding screen number. The concentration measured before the start of the experiment is given at the left of the Y-axis and labelled in red as F1, F2 or F3 depending on the well screen.

As demonstrated in the current research, pre-treatment with permanganate improves the efficiency of the system by reducing the background reactivity of the aquifer but poses risks regarding elevated manganese concentrations in the groundwater. To prevent this side-effect, other oxidative treatment than permanganate should be explored for the enhancement of SIR efficiency. The increase in efficiency resulting from oxidative treatments would be therefore be most expressed in systems with lower initial iron concentrations.

Furthermore, the current research was able to explain the lower efficiency of well 10 with regards to other wells. The strong variability of dissolved iron of the native groundwater with depth, with high concentrations in the deepest part of the wellscreen, results in very low recovery efficiencies. This responds to the fact that a good part of the oxygen (and a possible increase in available oxygen due to a pre-treatment like the one performed here) will be consumed to oxidize the high Fe^{2+} concentrations measured in deeper part of the area surrounding the SIR well. With the installment of SIR wells, variable iron concentrations in the aquifer with depth should be considered. To maximize SIR efficiency, where possible extraction from depths with high iron concentrations, even thin, should be avoided.

4 Conclusions

Subsurface iron removal systems are an efficient and natural way of reducing the iron and manganese concentrations in abstracted groundwater. These systems have been in operation for decades but in this study the understanding of the controls on their efficiency and of the options for optimization has improved.

In the current research, two different experiments were carried out by which the reactivity of the sediment surrounding two different SIR wells was tested. During the test at well 3 double the usual volume of oxygen-enriched water was infiltrated in the best performing well of the well field. This resulted in oxidation of fresh, previously unoxidized sediment. Contrary to expectations, this did not lead to a lowering of the removal efficiency. Instead, the recovery efficiency of the SIR well that could be achieved was much higher than the operational efficiency. In part this could be due to the formation of new iron and manganese oxides that provide more sorption area for inflowing iron and manganese. In largest part however, it seems that the operational efficiency maintained thus far was suboptimal as a doubled efficiency could be reached. The manganese concentrations however were not greatly influenced by this experiment since any precipitated manganese oxides will be reduced by inflowing iron and result in increasing concentrations (Fig. 3-3)

During the test at well 10 double the usual volume of water was infiltrated with the addition of a concentrated NaMnO4 solution. The permanganate was used to oxidize the sedimentary phases (organic matter, pyrite) to reduce the background reactivity of the aquifer. This resulted in reduced competition for oxygen and slightly higher efficiencies for that well despite the initial high iron concentrations in the deeper part of the aquifer. These high concentrations and the heterogeneity in the background reactivity explained the low observed iron removal efficiencies to date for this well. However, the permanganate treatment resulted in high abstracted manganese concentrations for a long period. Therefore the possibilities for using alternative oxidation methods for pretreatment should be explored. In addition, to increase overall removal efficiencies the possibilities for shortening the well screen length to avoid the abstraction of deeper groundwater, rich in iron, should be explored since the iron concentrations are the factor that determines the maximum removal efficiency that can be achieved.

Groundwater monitoring after the interaction of permanganate with the aquifer sediment indicated the presence of some trace metals and elements in the infiltrated permanganate solution, but did not indicate that mobilization or immobilization resulted in any significant irreversible changes in the trace metals and elements content. This was in keeping with the results from sediment testing. Also, their concentrations in abstracted groundwater remained below drinking water standards during the experiment .

The maximum achievable SIR efficiency is determined by the iron concentrations in the groundwater. Therefore, for two wells that can be operated at the same efficiency, the efficiency of the well with lower iron concentrations can be increased further than for the well with higher iron concentrations. This improved efficiency can result from continued operation over time or from pre-oxidative treatment to remove background reactivity.

The insights from earlier modeling results provided a good basis for anticipating and exploring the results of the field tests. However, the field tests have highlighted complexities and interactions that occur during SIR, that go beyond the capability of the SIR model developed thus far. For the current SIR models to be more accurate in describing site-specific conditions, particularly the capacity to include vertically variable iron concentrations in the inflowing groundwater and the interaction between manganese and iron needs to be incorporated.

Increasing the oxygen concentration of the infiltrated water was already an operational measure that was applied at the studied well field Corle. With respect to further operational optimization, this research has shown that the efficiencies with which SIR can be operated are to be expected to increase with time. Therefore regular monitoring of actual iron breakthrough at the well during abstraction can allow to improve the operational efficiency. In addition, it was shown that the oxidative treatment of the aquifer sediment surrounding the SIR well can be used to improve the SIR efficiency. Finally, rather than focusing on iron concentrations in bulk abstracted groundwater, for optimal SIR efficiency it was shown that locally high iron concentrations zones with depth in groundwater have a strong negative impact on overall SIR well efficiency.

5 Literature

Antoniou, E.A., Hartog, N., van Breukelen, B.M., Stuyfzand, P.J. 2014. Aquifer pre-oxidation using permanganate to mitigate water quality deterioration during aquifer storage and recovery. Applied Geochemistry 50 (2014) 25–36.

Appelo, C., Drijver, B., Hekkenberg, R. and Jonge, M.d. (1999) Modeling in situ iron removal from ground water. Groundwater 37, 811–817.

Appelo, C.A.J. and Vet, W.W.J.M. (2003) Modeling in situ iron removal from groundwater with trace elements such as As, in: Welch, A., Stollenwerk, K. (Eds.), Arsenic in Ground Water. Springer US, pp. 381–401.

de la Loma, B. and Hartog, N. (2016) Subsurface Iron removal in historical field pilots, KWR Watercycle Research Institute.

Dzombak, D.A. and Morel, F.M. (1990) Surface complexation modeling: hydrous ferric oxide. John Wiley & Sons.

Hartog, N., Griffioen, J. and Van Bergen, P. (2005) Depositional and paleohydrogeological controls on the distribution of organic matter and other reactive reductants in aquifer sediments. Chemical Geology 216, 113–131.

Hartog, N., Van Bergen, P., De Leeuw, J. and Griffioen, J. (2004) Reactivity of organic matter in aquifer sediments: geological and geochemical controls. Geochimica et Cosmochimica Acta 68, 1281–1292.

Appendix

Results from the XRF analysis: metal oxides content in the sediment sediment samples.

Well		P03	P03	P03		P10	P10	P10	P10	P10	P10	P10
Sample		1	2	3		4	9 (KMnO4)	5	6	10 (KMnO4)	7	8
Depth-to		31 – 32 m	35 – 36 m	38 – 39 m		27 – 28 m	27 – 28 m	30 – 31 m	33 – 34 m	33 – 34 m	36 – 37 m	38 – 39 m
Al2O3	%	2.46	1.06	1.36		3.9	3.72	2.08	2.12	2.06	1.04	1.08
BaO	%	0.04	0.02	0.02		0.04	0.05	0.04	0.04	0.04	0.03	0.03
CaO	%	1.5	3.73	5.27		5.88	5.18	1.06	1.62	1.34	2.49	3.34
CoO	%	<0,02	<0,02	<0,02		<0,02	<0,02	<0,02	<0,02	<0,02	<0,02	<0,02
Cr2O3	%	<0,02	<0,02	<0,02		<0,02	<0,02	<0,02	<0,02	<0,02	<0,02	<0,02
CuO	%	<0,02	<0,02	<0,02		<0,02	<0,02	<0,02	<0,02	<0,02	<0,02	0.04
Fe2O3	%	1.48	1.88	1.7		1.24	1.1	0.72	1.07	0.84	1.62	2
K2O	%	0.98	0.36	0.42		1.39	1.36	0.82	0.82	0.85	0.43	0.4
MgO	%	0.22	0.31	0.44		0.68	0.6	0.19	0.24	0.21	0.22	0.22
Mn3O4	%	0.02	0.02	0.03		0.04	0.09	0.02	0.05	0.13	<0,02	0.02
MoO3	%	0.02	<0,02	0.02		0.02	0.02	0.03	0.02	<0,02	<0,02	0.04
Na2O	%	0.37	0.14	0.19		0.76	0.72	0.3	0.3	0.3	0.12	0.1
Nb2O5	%	<0,02	<0,02	<0,02		<0,02	<0,02	<0,02	<0,02	<0,02	<0,02	<0,02
NiO	%	<0,02	<0,02	<0,02		<0,02	<0,02	<0,02	<0,02	<0,02	<0,02	<0,02
P2O5	%	0.11	0.07	0.08		0.05	0.05	0.05	0.08	0.06	0.07	0.07
PbO	%	0.02	0.03	0.02		0.02	0.02	0.02	0.02	0.02	0.02	0.02
SO3	%	0.1	1.94	1.6		0.06	0.02	0.04	0.1	0.1	0.71	0.46
SiO2	%	90.84	87.44	84.1		80.25	81.98	93.26	91.48	92.43	90.44	88.52
SnO2	%	<0,02	<0,02	<0,02		<0,02	<0,02	<0,02	<0,02	<0,02	<0,02	<0,02
SrO	%	0.02	<0,02	0.02		0.02	0.02	<0,02	<0,02	<0,02	<0,02	0.03
Ta2O5	%	<0,02	<0,02	0.02		<0,02	<0,02	0.02	0.02	0.02	<0,02	<0,02
TiO2	%	0.09	0.06	0.06		0.17	0.16	0.08	0.08	0.07	0.06	0.06
V2O5	%	<0,02	<0,02	<0,02		<0,02	<0,02	<0,02	<0,02	<0,02	<0,02	<0,02
WO3	%	0.03	0.03	0.04		0.03	0.02	0.04	0.03	0.04	0.06	0.05
ZnO	%	<0,02	<0,02	<0,02		<0,02	<0,02	<0,02	<0,02	<0,02	<0,02	<0,02
ZrO2	%	<0,02	<0,02	<0,02		0.02	0.02	<0,02	<0,02	<0,02	<0,02	<0,02